# KSHV infection of endothelial precursor cells with lymphatic characteristics as a novel model for translational Kaposi's sarcoma studies

Krista Tuohinto[1¶], Terri A. DiMaio[2¶], Elina A. Kiss[1], Pirjo Laakkonen[1,3], Pipsa Saharinen[1], Tara Karnezis[4], Michael Lagunoff[2*] and Päivi M. Ojala[1*]

[1] Translational Cancer Medicine Research Program, Faculty of Medicine, University of Helsinki. Finland.

[2] Department of Microbiology, University of Washington. Seattle WA, United States of America.

[3] Wihuri Research Institute, Biomedicum Helsinki. Finland.

[4] Gertrude Biomedical Pty Ltd., Melbourne, Queensland, Australia.

* Co-corresponding authors: lagunoff@uw.edu, paivi.ojala@helsinki.fi

¶ These authors contributed equally to this work

# Abstract

Kaposi's sarcoma herpesvirus (KSHV) is the etiologic agent of Kaposi's sarcoma (KS), a hyperplasia consisting of enlarged malformed vasculature and spindle-shaped cells, the main proliferative component of KS. While spindle cells express markers of lymphatic and blood endothelium, the origin of spindle cells is unknown. Endothelial precursor cells have been proposed as the source of spindle cells. We previously identified two types of circulating endothelial colony forming cells (ECFCs), ones that expressed markers of blood endothelium and ones that expressed markers of lymphatic endothelium. Here we examined both blood and lymphatic ECFCs infected with KSHV. Lymphatic ECFCs are significantly more susceptible to KSHV infection than the blood ECFCs and maintain the viral episomes during passage in culture while the blood ECFCs lose the viral episome. Only the KSHV-infected lymphatic ECFCs grew to small multicellular colonies in soft agar whereas the infected blood ECFCs and all uninfected ECFCs failed to proliferate. The lymphatic ECFCs express high levels of SOX18, which supported the maintenance of high copy number of KSHV genomes. When implanted subcutaneously into NSG mice, the KSHV-infected lymphatic ECFCs persisted in vivo and recapitulated the phenotype of KS tumor cells with high number of viral genome copies and spindling morphology. These spindle cell hallmarks were significantly reduced when mice were treated with SOX18 inhibitor, SM4. These data suggest that KSHV-infected lymphatic ECFCs can be utilized as a KSHV infection model for in vivo translational studies to test novel inhibitors representing potential treatment modalities for KS.


**Keywords:**

KSHV; HHV-8; lymphatic endothelium; ECFCs; Endothelial precursor cells; Kaposi's sarcoma; SOX18

**Author summary:**

Kaposi's sarcoma herpesvirus (KSHV) is the etiologic agent of Kaposi's sarcoma (KS). The main proliferative component of KS, spindle cells, express markers of lymphatic and blood endothelium. Endothelial precursor cells, which are circulating endothelial colony forming cells (ECFCs), have been proposed as the source of spindle cells. Here we examined both blood and lymphatic ECFCs infected with KSHV. Lymphatic ECFCs are readily infected by KSHV, maintain the viral episomes and show minimal transformation of the cells, which the infected blood ECFCs and all uninfected ECFCs failed to show. The lymphatic ECFCs express SOX18, which supported the maintenance of high copy numbers of KSHV genomes. The KSHV-infected lymphatic ECFCs persisted in vivo and recapitulated the phenotype of KS tumor cells such as high number of viral genome copies and spindling morphology. These KS tumor cell hallmarks were significantly reduced by SOX18 chemical inhibition using a small molecule SM4 treatment. These data suggest that KSHV-infected lymphatic ECFCs could be the progenitors of KS spindle cells and are a promising model for the translational studies to develop new therapies for KS.

# Introduction

Kaposi's sarcoma herpesvirus (KSHV) is a gamma herpesvirus and the etiologic agent of Kaposi's sarcoma (KS) as well as rare B-cell proliferative diseases primary effusion lymphoma and AIDS-associated Castleman's disease. KS is a hyperplasia consisting of enlarged malformed vasculature and spindle-shaped cells which are the main proliferative component of KS. Spindle cells express markers consistent with an endothelial cell origin [1–5].

Endothelial cells are largely divided into blood vascular and lymphatic endothelial cells. While closely related, the cells making up the blood and lymphatic vasculatures have distinct functions and express specific markers. KS spindle cells express several markers specific to lymphatic endothelium though they also express markers of blood endothelium. However, it has been shown that KSHV infection of endothelial cells in culture induce changes in endothelial cell marker expression. Specifically, KSHV infection of blood vascular endothelial cells (BEC) induces changes consistent with lymphatic differentiation including induction of PROX1 and vascular endothelial growth factor 3, VEGFR3 expression [6–8]. However, infection of lymphatic endothelial cells (LEC) induces the expression of VEGFR1, consistent with its expression in BEC. Therefore, the contribution of these cell types to development of KS tumors is unclear. Another feature of spindle cells is the expression of mesenchymal cell markers, an observation that has prompted the idea that undifferentiated mesenchymal cells might be a cell type of origin [9]. This hypothesis remains elusive since the mesenchymal phenotypes could also emerge due to Endothelial-to-Mesenchymal-Transition (EndMT) induced by KSHV-infection of LECs [10,11].

KS tumors develop primarily in the skin of patients with classic KS. More aggressive AIDS-associated KS can infiltrate internal organs. However, KS is not found in tissues lacking lymphatic vasculature, such as parenchyma and retina. This suggests that LECs are a necessary component of KS development. Furthermore, we and others have previously found that LECs are more susceptible than BECs to KSHV infection [8,12–15]. The KSHV-infected primary human LECs (K-LECs) display a unique infection program characterized by maintenance of high KSHV genome copies, spontaneous lytic gene expression and release of significant amounts of infectious virus [12,13]. This is in striking contrast to BECs and other

KSHV-infected in vitro cell models. KSHV infection of neonatal LECs but not BECs allows them to bypass replicative senescence [14]. However, KSHV-infected LECs, like KS spindle cells, are not fully immortalized. Whether LECs are a reservoir for KSHV *in vivo* has yet to be determined.

Endothelial colony forming cells (ECFCs) are circulating cells thought to be endothelial precursors. Previous studies have shown that circulating endothelial precursor cells home to sites of neoangiogenesis [16,17]. However, the contribution of precursor cells to neoangiogenesis is unclear. Previous investigations suggest that circulating endothelial precursors could be important for the development of KS lesions. One study found that KS lesion formation following kidney transplant occurred in distal extremities [18]. Importantly, the spindle cells of the KS tumors were gender matched to the transplanted tissue, not the recipient, suggesting the presence of circulating cells harboring KSHV. Further studies have isolated ECFCs from patients with classic KS, which were found to be positive for KSHV DNA [19]. Interestingly, KSHV infection of endothelial progenitor cells isolated from umbilical cord blood reduces their angiogenic potential [20]. It has been previously proposed that KSHV infected ECFCs could be the source of spindle cells seeding the KS tumors [19–21].

We previously isolated ECFCs from whole blood and found that there are two types of ECFCs [22]. The predominant ECFC expressed markers of blood endothelial cells as has been previously described [23–25]. Importantly, we identified rare ECFC isolates expressing markers of the lymphatic vasculature. Our recent results show that the key developmental lymphatic transcription factor (TF), SOX18, is expressed in KS tumors and needed to support a unique KSHV infection program with high number of intracellular KSHV genome copies in infected human LECs. SOX18 binds to the origins of KSHV replication and

increases the intracellular viral DNA genome copies [12]. Depletion by RNAi or specific inhibition of SOX18 homo- and heterodimerization by a small molecule inhibitor SM4 or R-propranolol [26,27] dramatically decreases both intracellular viral genome copies and release of infectious virus, suggesting SOX18 as an attractive therapeutic target for KS.

Here, we show that similar to LECs, lymphatic ECFCs are more susceptible to KSHV infection and maintain the viral episome in contrast to blood ECFCs. KSHV infection of lymphatic ECFCs allowed proliferation, albeit limited, of these cells in soft agar, suggesting that KSHV may promote enhanced survival of lymphatic ECFCs. We further utilized the SOX18-expressing lymphatic ECFCs as a physiologically relevant KSHV infection model for testing the translational potential of SOX18 small molecule inhibitor SM4 in vitro and in vivo. Together, these data suggest that circulating lymphatic ECFCs could potentially represent virus reservoirs and putative precursors as the source for the initiation of KS tumors.

# Results

### Lymphatic ECFCs are more permissive to KSHV infection than blood ECFCs

We have previously shown that neonatal LECs are more susceptible to KSHV infection than BECs [12,14]. Also, we previously identified two types of ECFCs, ones that expressed markers of BEC and ones that expressed markers of LEC. To determine whether also these lymphatic ECFCs are more susceptible to KSHV-infection than blood ECFCs, we seeded both cell types onto 6-well plates, allowed them to adhere, and followed by infection with identical dilutions of KSHV at either a high or low MOI. After two

128 days, we harvested the cells and performed immunofluorescence for viral latency-associated nuclear
129 antigen (LANA) expression and counted the percentage of cells that were latently infected. As shown
130 in Fig 1A, at high MOI, 98% of lymphatic ECFCs are infected, while only 87% of the blood ECFCs are
131 infected. At high MOI, each cell may have multiple instances of infection, therefore counting the
132 percentage of LANA+ cells may miss cases of superinfection. To address this, we performed the same
133 experiment with a low MOI. Fig 1B shows that lymphatic ECFCs are infected at almost three times the
134 rate of blood ECFCs.
135
136 We also isolated ECFCs using a different protocol where the cells were isolated from the whole blood
137 of four, additional healthy donors, but as an adherent subpopulations rather than from single cell
138 colonies. By fluorescence associated cell sorting (FACS) analyses these cells expressed substantial levels
139 of CD34, VEGFR3, podoplanin, CD31/PECAM1, PROX1 and SOX18, suggesting that they also represent
140 predominantly lymphatic ECFCs (S1 Fig), not blood vascular endothelial ECFCs. Next, we analyzed if
141 these lymphatic ECFCs could support spontaneous lytic replication and production of new infectious
142 viruses, unique to KSHV-infected LECs, but not seen in BECs [12,13]. To this end, we compared the
143 infection of primary human LECs, BECs and the lymphatic ECFCs with recombinant rKSHV.219 [28] on
144 6-well plates and the infection was followed up for 2 weeks. Fig 1C shows latent infection (indicated by
145 GFP expression) in all cell types, however, the spindling phenotype became visible in 7 days post
146 infection only in lymphatic ECFCs (K-ECFCLY) and K-LECs, but not in K-BECs. Spontaneous lytic
147 replication (indicated by RFP expression) was observed both in K-ECFCLYs and K-LECs, albeit more
148 prominent in K-LECs but not seen in K-BECs. Accordingly, as shown in Fig 1D, in addition to GFP and the
149 latent protein LANA, K-ECFCLY expressed the viral lytic protein K8.1. We have previously shown that

K8.1 is prominently expressed by K-LECs, but not in K-BECs [12]. Accordingly, K-BECs did not produce infectious virus, whereas K-ECFCLYs did albeit significantly less than K-LECs (Fig 1E). Similar results showing that K-ECFCLYs can produce infectious virus were obtained when using lymphatic ECFCs from three additional donors (S2 Fig). This indicates that lymphatic ECFCs are permissive to KSHV infection and capable to support productive, lytic replication.

**Lymphatic ECFCs maintain the KSHV viral episome**

The KSHV genome is maintained as an episome in dividing cells, though this process is not robust, and the episome is lost over time in cultured endothelial cells [29–32]. Our previous data with neonatal ECs showed that LECs were able to maintain the KSHV episome but BECs lost the genome relatively rapidly over the course of cell passaging [12,14]. To test whether the rate of loss is different between blood and lymphatic ECFCs, we infected cells with KSHV and harvested them every two days for immunofluorescence for LANA expression. Because lymphatic ECFCs are more susceptible to KSHV infection, we used higher MOI to the blood ECFCs to achieve similar initial infection rates. By using LANA staining as a surrogate marker for genome copies, Fig 1F shows that, although in the beginning very similar infection rates were observed for both blood and lymphatic ECFCs, the blood ECFCs gradually lose the episome and by ten days post infection fewer than 40% of cells exhibited punctate LANA staining. In contrast, the lymphatic ECFCs maintained infection at almost 100%.

Additionally, primary LECs and BECs and the lymphatic ECFCs isolated as subpopulation were infected with KSHV using low MOI and harvested for total DNA isolation at days 3, 7, 10 and 14 post infection. Quantification of KSHV genome copies demonstrates that lymphatic ECFCs, similar to LECs, maintain

the viral episomes (Fig 1G). Interestingly, K-ECFCLYs and K-LECs show even an increase in genome copies until day 14. In contrast, by using low MOI, K-BECs achieve a lower number of genome copies which are gradually lost within two weeks after infection (Fig 1G).

**KSHV inhibits proliferation but not tube formation of ECFCs**

To determine if KSHV confers a growth advantage to ECFCs, we mock-or KSHV-infected blood and lymphatic ECFCs and seeded $3x10^4$ cells 48 hours post infection in 6-well plates and monitored their confluence over time using the live-cell Essen Bioscience IncuCyte imaging system. Fig 2A shows that mock-infected blood ECFCs proliferated at a slightly higher rate than mock-infected lymphatic ECFCs. Interestingly, KSHV infection significantly reduced proliferation of both blood and lymphatic ECFCs. However, there are no significant differences in the reduction of proliferation between these two cell types suggesting that KSHV has a mild inhibitory effect on cell proliferation, but this is not dependent on blood versus lymphatic cell origin. We then also compared the proliferation rate of KSHV-infected and non-infected lymphatic ECFCs that had been isolated as a subpopulation by seeding cells to 96-well plates and subjected them to an EdU pulse for 4h before fixation. The Click-IT EdU staining, measured only from LANA+ cells, indicated only slight difference between the percentage of uninfected and the KSHV-infected lymphatic ECFCs undergoing proliferation (Fig 2B), confirming the mild inhibitory effect on cell proliferation.

To determine if KSHV-infection supports viability of lymphatic ECFCs under limited growth factor conditions, mock and KSHV-infected cells were seeded on 96-well plates. The cells were grown either in normal media containing all the supplements, growth factor reduced media or media without any

194 supplements or serum for 7-day period (media replenished at day 4). As shown in Fig 2C, KSHV-infected
195 lymphatic ECFCs survived better than the mock cells under both the growth factor reduced and serum
196 deprived conditions, indicating increased viability in limiting growth media.
197
198 KS tumors are highly vascularized with irregular, enlarged vascular slits, indicating increased
199 neovascularization. We have previously shown that KSHV infection of ECs promotes the stability of
200 capillary networks in a Matrigel model of endothelial cell migration [33]. To measure whether KSHV
201 alters the ability of blood or lymphatic ECFCs to undergo angiogenesis, we mock- or KSHV-infected
202 blood and lymphatic ECFCs. Cells were plated on a Matrigel matrix 48 hours post infection. Fig 2D shows
203 that both blood and lymphatic ECFCs organized into networks on Matrigel at 4 hours post plating (top
204 panels). Interestingly, unlike mature endothelial cells, both blood and lymphatic ECFCs maintained the
205 cord structures at 24 hours post plating (bottom panels). Under these conditions, KSHV had little effect
206 on the ability of ECFCs to organize on Matrigel and maintain their capillary stability.
207
208 **KSHV confers a survival advantage to lymphatic ECFCs grown in soft agar**
209 We next examined if KSHV promotes anchorage independent growth of ECFCs in soft agar, an
210 indicator of cell transformation. We mock- or KSHV-infected blood and lymphatic ECFCs and, after 48
211 hours, embedded a single cell suspension in a soft agar matrix which was overlaid by normal growth
212 media. We then monitored the growth and formation of small colonies of cells over the course of four
213 weeks. Fig 3A shows images of cell suspensions following four to five weeks of growth. We could not
214 find any evidence of multicellular colonies in the uninfected blood nor lymphatic ECFCs. Only single cells
215 could be visualized even when incubated 36 days indicating these cells are unable to proliferate in the

absence of attachment to a solid surface. Additionally, KSHV-infected blood ECFCs (K-ECFCBL) showed no indication of multicellular colonies in soft agar. Interestingly, after four weeks in soft agar culture, many multi-cellular colonies were found in the wells containing K- ECFCLYs indicating the ability of KSHV infected lymphatic ECFCs to grow in an anchorage independent fashion. Scanning and quantifying multiple experiments indicated that approximately 10% of the KSHV infected ECFCLYs formed multicellular colonies (Fig 3B).

The capacity of KSHV-infected cells to grow in soft agar was also addressed using the lymphatic ECFCs isolated as an adherent subpopulation. To this end, non-infected and KSHV-infected lymphatic ECFCs from four different donors were embedded as single cells to soft agar seven days post infection. Fully transformed renal cell carcinoma cell line stably infected with KSHV, iSLK.219 [34], was used as a positive control. We then monitored the growth and formation of small colonies of cells over the course of four weeks. Fig 3C shows images of cells from donor 1 after four weeks of growth. The colonies were calculated and quantified as shown in Fig 3D-E. We could not detect any evidence of multicellular colonies in the non-infected samples, however, after four weeks in soft agar, many colonies were observed in the wells containing K-ECFCLYs. These results further support the ability of KSHV infected lymphatic ECFCs to proliferate in an anchorage independent fashion.

Together, this suggests that KSHV may promote the survival and proliferation of lymphatic ECFCs but not blood ECFCs in soft agar. However, this effect was limited to small colonies containing approximately 3-17 cells. Fully transformed cells like iSLK.219 form robust colonies with 100s of cells (Fig 3C-D). Therefore, KSHV allows significant but limited proliferation of cells in soft agar indicating

minimal transformation of the cells. The slow expansion of K-ECFCLYs in soft agar as compared to the iSLK.219 cell line would be consistent with the slower growth of KS tumors compared to many more aggressive tumors like renal cell carcinoma.

**Gene expression changes induced by KSHV infection of lymphatic ECFCs**

To determine the effects of KSHV infection on blood and lymphatic ECFCs, we measured the global gene expression differences between these cells upon primary KSHV infection. mRNA from blood and lymphatic ECFCs that were mock- or KSHV-infected, was analyzed by high throughput RNA sequencing 48 hours post infection. We also compared these gene expression profiles to previous data we generated from mature BECs and LECs [14]. S3A Fig shows a Venn diagram comparing all genes upregulated during KSHV infection by at least 2-fold in all cell types. Approximately 125 genes are specific to KSHV-infected BECs (both mature and ECFCs), while 52 genes were specific to LECs. To validate the RNA-sequencing results, we analyzed selected genes that had differential expression between blood and lymphatic ECFCs using custom PrimePCR plates (S3B Fig). These data are consistent with the gene expression changes identified by high-throughput sequencing.

Using Cytoscape software and the Gene Ontology classification application BINGO, we determined the Gene Ontology terms that were highly enriched among the K-ECFCBLs and K-ECFCLYs. The most highly enriched categories for blood ECFCs are listed in S1 Table. Interestingly, these include many immune response categories. The individual genes for some of these categories are listed in S2 Table. In contrast, lymphatic ECFCs were not enriched in immune response categories, but were enriched in genes involved in cell differentiation and signaling (S3 & S4 Tables). To confirm whether genes involved in the

innate immune response are upregulated in KSHV-infected blood ECFCs but not lymphatic ECFCs, we performed real-time quantitative RT-PCR on RNA from mock and KSHV infected blood and lymphatic ECFCs. S3C Fig shows that several genes involved in innate immunity, such as viperin and IFI6, are induced by KSHV in blood ECFCs but not in lymphatic ECFCs. This suggests that lymphatic and blood ECFCs may have differential innate immune responses to KSHV infection.

High-throughput RNA sequencing was repeated with lymphatic ECFCs, isolated as a subpopulation from a different donor. Cells were mock- or KSHV-infected for seven days before total RNA was harvested for sequencing. The gene expression profiles were compared to the data obtained from lymphatic ECFCs infected with KSHV for 48h as described above. S3D Fig shows a Venn diagram of 1444 shared gene expression changes between the two infected ECFCLY-isolates, also listed in S6 Table. The higher number of differentially expressed genes with ECFCLYs infected for seven days is most likely due to the longer exposure to virus thus allowing more phenotypic changes to occur.

S3E Fig shows a Volcano blot of differentially expressed genes between mock and KSHV-infected ECFCLY after 7 days of infection. Interestingly, significantly upregulated genes include those involved in lymphatic endothelial specification, such as LYVE1, Podoplanin, and VEGFC. Also, some mesenchymal genes implicated in EndMT were moderately, but significantly, upregulated. Selected genes were validated with RT-qPCR shown in S3F Fig, and they are consistent with the gene expression changes identified by high-throughput sequencing.

**SOX18 inhibition reduces the hallmarks of KSHV infection in lymphatic ECFCs in vitro and in vivo**

Our recent data demonstrated that SOX18, expressed abundantly in KS tumors and K-LECs, binds to the origins of KSHV replication and increases the intracellular viral DNA genome copies [12]. To address the SOX18 role in K-ECFCLYs the cells were treated with siRNA targeting SOX18 or non-targeting control siRNA (siNeg) after five days of infection and analyzed three days later for KSHV genome copies, number of LANA positive cells and infectious virus release on naïve U2OS cells (Fig 4A-D). Similar to K-LECs, depletion of SOX18 significantly reduced the intracellular viral genome copies, number of LANA-positive cells and the virus titers (Fig 4A-D). To measure the effect of SOX18 inhibition by the SM4 inhibitor on lymphatic K-ECFCLYs, GFP and RFP positive cells (to monitor latent and lytic infection), spindling phenotype of the cells, in addition to the above-mentioned phenotypes were measured as the hallmarks of KSHV infection. K-ECFCLYs (at 5 days p.i.) were treated with SM4 at concentrations 1 µM, 25 µM and 50 µM for 6 days and DMSO was used as a control. Fig 4E shows that similarly to depletion of SOX18 by siRNA, 25 µM of SM4 was sufficient to reduce the GFP positive cells, spindling phenotype and RFP signal indicating cells undergoing lytic cycle. Furthermore, SM4 significantly, and in a dose-dependent manner, reduced the number of KSHV genome copies, LANA positive cells and released infectious virus from the infected lymphatic ECFCs (Fig 4F-H). These data demonstrate that SOX18 is required to maintain the high number of intracellular KSHV genomes and viral titers in the K-ECFCLYs, similar to K-LECs [12].

By using a three-dimensional (3D), organotypic cell model for KSHV infection we have previously shown that KSHV promotes the ability of mature lymphatic endothelial cells to invade into 3D cross-linked fibrin [10]. Next, we tested if KSHV infection would induce the 3D sprouting growth of the lymphatic ECFCs and if it was dependent on SOX18 function. To this end, mock- and KSHV-infected lymphatic

304 ECFCs cells were first allowed to form spheroids overnight and then embedded in 3D fibrin. As shown
305 in Fig 4I KSHV induced outgrowth of sprouting cells from the lymphatic ECFC spheroids, which was
306 completely abolished during the 6-day 50 µM SM4 treatment. The mock infected lymphatic ECFC
307 spheroids did not sprout and SM4 did not have any effect on their morphology (Fig 4J). Together these
308 data support that the lymphatic ECFC represent a viable model for KSHV infection and testing of the
309 translational potential of novel targets for KS.
310
311 **SOX18 inhibition reduces the hallmarks of KSHV infection in vivo**
312 As the KSHV-infected lymphatic ECFCs support the complete lytic replication program,
313 proliferate, and show emerging transformation, we decided to test their long-term persistence *in vivo*
314 in NSG mice when implanted subcutaneously. Mock and KSHV-infected lymphatic ECFCs were
315 implanted subcutaneously in Matrigel after seven days of infection (7 d.p.i.). After a 30-day period,
316 visible cell plugs were collected and analyzed for the presence of KSHV DNA and intensity of GFP (from
317 the rKSHV.219 latent infection) and LANA by IFA from the paraffin embedded sections (Fig 5A). Fig 5B
318 shows that the K-ECFCLYs recapitulate the spindling phenotype of KS tumor cells in the lesions and
319 express LANA suggesting that they represent a promising *in vivo* model to investigate the potential
320 treatment modalities for KS.
321
322 We next tested the effect of SM4 on similar model (Fig 5A). To this end, 4x10^$^{6}$ mock- or KSHV infected
323 lymphatic ECFCs, mixed with K-LECs, were injected subcutaneously into NGS mice 7 d.p.i. K-LECs were
324 included to provide more spontaneously lytic cells that can contribute to the inflammatory
325 microenvironment and produce more infectious virus. The final proportions of cells were 90-95% of K-

ECFCLYs and 5-10% of K-LECs. The next day SM4 or vehicle (80% PEG-400, 10% Solutol HS-15, 10% dH2O) was administered orally at a dose of 25mg/kg of body weight daily for 10 sequential days as described in [27], after which the cell plugs were collected and analyzed by IHC for cell morphology, IFA for KSHV infection, and qPCR for KSHV DNA.

Interestingly, IHC of cell plugs from mice treated with SM4 displayed several necrotic areas in the grafts, whereas the vehicle group showed cells with a spindle-like, elongated morphology, often found in clusters (Fig 5C, left panels). IFA was performed for sections to distinguish the GFP-expressing, KSHV-infected cells with spindle-like morphology. Stained sections imaged with a confocal microscope are shown in Fig 5C (right panels). The intensity of GFP signal and the coverage of spindling cells in the sections differed significantly between the treatment groups (Fig 5D). While GFP signal in spindling cells was observed in the Vehicle group, the overall GFP signal in the SM4 group was weak, having also significantly less cells with spindling morphology. Quantification showed that the Vehicle group had higher GFP intensity and more spindling cells, when normalized to the section area, and when compared to the SM4 treatment group (Fig 5D). The mock infected lymphatic ECFCs did not express GFP and were used to subtract the autofluorescence for quantification. These results indicate strong potential of SOX18 inhibition to reduce the hallmarks of KSHV infection in this novel in vivo KSHV infection model.

We next measured the KSHV genome copy numbers by qPCR from the extracted total DNA of the grafted samples. The human repetitive ALU-sequences as an internal control were used as a highly sensitive and specific quantification for the human cells among the abundant rodent cells. The KSHV

genome copies were quantified using primers specific for LANA. Fig 5E shows that SM4 significantly decreased the relative KSHV genome copy numbers compared to the Vehicle control group further supporting the potential of SOX18 inhibition as a viable therapeutic modality for KS.

## Discussion

Studies of KS tumors are limited by the lack of a clear understanding of the source of the main proliferating tumor cell, the spindle cell. While spindle cells express markers of lymphatic endothelium and most closely align to the gene expression pattern of lymphatic endothelial cells, they also express blood vascular endothelial and mesenchymal cell markers. However, in contrast to angiogenic endothelial cells, quiescent endothelial cells in mature vessels generally do not migrate. There is evidence that the cells that seed KS tumors are able to traffic from the kidney as KS of donor origin formed to the lower extremities of the recipient following a kidney transplant from a KSHV-positive donor [18]. Interestingly, endothelial precursor cells traffic throughout the body through the blood and are known to traffic to sites of angiogenesis. Thus, it has been proposed by multiple groups that endothelial precursor cells are a likely source of KS spindle cells [19–21]. Therefore, we sought to isolate the precursor ECFCs and characterize KSHV infection in those cells. When isolating ECFCs from human blood, we found that the standard endothelial colony forming cells could be separated into isolates that expressed blood endothelial markers and isolates that expressed lymphatic specific markers. We also isolated ECFCs from four donors as an adherent subpopulation without clonal expansion of individual colonies. Interestingly, these isolates represented uniform cultures of predominantly lymphatic ECFCs.

368 This might indicate that lymphatic ECFCs have a growth advantage over the blood ECFCs and take over
369 the culture when cells proliferate during colony formation.
370
371 Similar to the neonatal blood and lymphatic endothelial cells isolated from foreskins, the lymphatic
372 ECFCs were more permissive to KSHV infection and the viral episomes were maintained over multiple
373 passages at higher levels as compared to the blood ECFCs. KSHV infection did not alter the ability of
374 either cell type to form capillary-like structures in Matrigel indicating that KSHV does not dramatically
375 alter the angiogenic potential of either cell type. However, infection with KSHV slightly decreased the
376 proliferation rate of both blood and lymphatic ECFCs. We have also noted a decrease in proliferation of
377 neonatal and adult endothelial cells [12], so this appears to be a common phenotype of KSHV infection
378 of endothelial cells in general (DiMaio and Lagunoff, unpublished).
379
380 To determine if there was any evidence of transformation of the ECFCs despite the reduced
381 proliferation, we examined the proliferation of non-infected and infected blood and lymphatic ECFCs
382 following detachment from a solid matrix. Interestingly, neither non-infected or infected blood ECFCs
383 proliferated in soft agar nor did the uninfected lymphatic ECFCs. However, in a large number of studies
384 using six different isolates of KSHV-infected ECFCLYs, approximately 10% of the cells formed small
385 colonies following incubation of over four weeks in soft agar. While the colonies did not expand beyond
386 the small 3-17 cell colonies, in all the experiments performed we did not detect any colony formation
387 in the non-infected blood or lymphatic ECFCs or the infected blood ECFCs indicating that this
388 proliferation only occurred in the KSHV-infected lymphatic ECFCs and was reproducible. While there
389 were numerous colonies formed, not every cell formed a colony. Thus, the transformation phenotype

was limited while a similar assay with iSLK.219, a renal cell carcinoma cell line stably infected with a recombinant KSHV, led to very large colonies in soft agar of hundreds of cells or more. The iSLK.219 cells also formed colonies more rapidly. Of note, in line with our findings, KS tumors are fairly indolent and do not grow rapidly.

To begin to decipher why there are differences in the behavior of lymphatic and blood ECFCs following KSHV infection we performed RNAseq analysis of non-infected and KSHV-infected lymphatic and blood ECFCs. We identified 758 genes that are enriched in KSHV-infected blood ECFCs compared to lymphatic ECFCs (S5 Table). In contrast, 1,395 genes are enriched in lymphatic ECFCs. Interestingly, when we analyzed the lists of genes for enrichment of Gene Ontology categories, we found that many of the genes induced by KSHV in blood ECFCs were involved in the innate immune response. These include MX1 and MX2, which are interferon-induced genes that are viral restriction factors. MX2 in particular has been shown to be effective at inhibiting herpesviruses, including KSHV [35,36]. Other interferon response genes are also enriched in KSHV-infected blood ECFCs such as IFI6 and RSAD2. It is unclear what effect this enhanced interferon response has on blood ECFCs. However, it could play a role in the reduced susceptibility of blood ECFCs to KSHV infection or the increased rate of episome loss. We previously found that in neonatal LECs STING was not activated [37]. Further work is necessary to determine if the same is true for lymphatic ECFCs. In contrast to the blood ECFCs, genes upregulated by KSHV in lymphatic ECFCs were found to be involved in lymph vessel development and intracellular signaling. What role these genes have on KSHV infection of lymphatic ECFCs remains to be elucidated.

We recently reported high SOX18 expression in KS tumors and that was required to maintain the high number of intracellular KSHV genome copies in infected LECs, suggesting SOX18 as an attractive therapeutic target for KS [12]. Similar to K-LECs we found that KSHV-infected lymphatic ECFCs express high levels of SOX18 and inhibition of SOX18 by a specific small molecule inhibitor SM4 significantly reduced the intracellular viral genome copies also in KSHV-infected EFCFLYs. Since K-LECs do not support long-term growth in culture and do not show even emerging signs of transformation they cannot be used in preclinical in vivo studies to test the efficacy of SOX18 inhibitors. Therefore, we investigated whether KSHV-infected lymphatic ECFCs engrafted into NSG mice could serve as a physiologically relevant infection model to test the potential of SOX18 inhibition as a therapeutic modality for KS. The KSHV-infected ECFCLYs survived as xenografts in mice for at least a month and recapitulated the hallmarks of KSHV infection, which were significantly reduced upon SOX18 inhibition by SM4.

Together our data suggest that lymphatic ECFCs are more susceptible to KSHV infection and may have increased survival and proliferation capabilities during infection. While this does not definitively solve the issue of the source of spindle cells, it shows that infected lymphatic ECFCs are certainly a possible source. Moreover, our data supports that lymphatic ECFCs represent a viable new in vivo model for KSHV infection, suitable for translational studies testing new therapeutic approaches for KS. Further work to analyze KSHV infection of lymphatic ECFCs is warranted.

# Materials and Methods

## Cells

For isolation of ECFCs the blood samples were obtained from the Puget Sound Blood Bank (Seattle, WA, USA) as either outdated whole blood (approximately 500 ml per unit) or leukocyte reduction filters, which yielded between 4-7x$10^8$ leukocytes after elution. Whole blood was mixed 1:2 with phosphate-buffered saline (PBS) containing 10,000 units per liter heparin and 0.02% EDTA. Cells from leukocyte reduction filters were eluted with 200 ml PBS containing 10,000 units per liter heparin and 0.02% EDTA. ECFCs were then isolated and cultured as previously described [38]. Individual colonies of cells were clonally expanded. All experiments were performed on cells between passage 8 and 15.

For isolation of an adherent subpopulation of ECFCs fresh blood samples were obtained from the Finnish Red Cross Blood Services (Helsinki, Finland) as buffy coat concentrates devoid of platelets. After dilution of 1:2 in PBS, the cells were isolated according to manufacturer's instructions suing SepMate tubes (STEMCELL Technologies, Cambridge, UK) and Ficoll-Paque density gradient media (GE Healthcare, Uppsala, Sweden). The final number of mononuclear cells separated from each donor's blood bag was approximately 1.5x$10^7$ cells/mL, yielding a total of 200 million cells. The cells were transferred onto a fibronectin 25 µg/mL (Sigma-Aldrich, St.Louis, USA) and 15 µg/mL rat tail collagen (Merck, St.Louis, USA) pre-coated cell culture 6-well plate with EBM-2 endothelial media supplemented with 10% FBS and a growth factor bullet kit (Lonza, Walkersville, USA) 3 mL/well. Cultures were followed up to three weeks, washing away any non-adherent cells and changing fresh supplemented EBM-2 media every other day. When populations of adherent, cobblestone-like cells resembling endothelial cells formed, they were split onto pre-coated 10 cm culture dishes without colony selection. These cells

were then frozen in Cryo-SFM freezing media (Promocell, Heidelberg, Germany) and stored in a liquid nitrogen tank prior to the phenotype analyses and using as an infection model. All experiments were performed on cells between passage 3 and 8.

Primary human dermal lymphatic and blood endothelial cells (LEC C-12216 and BEC C-12211; Promocell, Heidelberg, Germany) and neonatal dermal microvascular endothelial cells (hDMVEC) were maintained as monolayer cultures in EBM-2 medium (Lonza, Walkersville, USA) supplemented with 5% fetal bovine serum, vascular endothelial growth factor, basic fibroblast growth factor, insulin-like growth factor 3, epidermal growth factor, and hydrocortisone (EGM-2 media). Human osteosarcoma cell line U2OS (ATCC: HTB-96) was used as a naïve cell line to study KSHV infection kinetics and efficacy of infection in the virus release assays. This cell line is highly susceptible to KSHV infection. iSLK.219 [34] is an RTA - inducible renal-cell carcinoma SLK cell line, stably infected with a recombinant KSHV.219. U2OS and iSLK.219 were grown in DMEM (Lonza), supplemented with 10% FCS (Gibco), 1% L-glutamate (Gibco), and 1% penicillin/streptomycin (Gibco). iSLK.219 cells were also supplied with 10 µg/mL puromycin (Sigma), 600 µg/mL hygromycin B (Invitrogen), and 400 µg/mL G418 (Invitrogen). All cells were propagated in a humified incubator at standard conditions and primary cells were used until passage five. Cells were regularly tested negative for *Mycoplasma* (MycoAlert Mycoplasma Detection Kit, Lonza, Walkersville, USA).

**FACS analysis**

The ECFCs isolated as an adherent subpopulation were analyzed by FACS using the following fluorescently conjugated antibodies for endothelial surface markers: A647-Podoplanin, PE-VEGFR3,

476 A647-CD34 and PE-CD31 (Biolegend, San Diego, USA). For the nuclear EC markers, cells were fixed and
477 permeabilized with MetOH and stained with antibodies against PROX1 (rabbit) (Proteintech, Rosemont,
478 USA) and SOX18 (mouse) (Santa Cruz Biotechnology, Dallas, USA), followed by staining with secondary
479 antibodies conjugated to Alexa Fluor 488 and 594 stains (Life Technologies). All samples were analysed
480 with BD Accuri C6 flow cytometer using unstained cells or secondary antibody only treated controls.
481
482 **Immunoblotting**
483 Cell lysis, SDS-PGE and immunoblot were performed as described in [39]. The following primary
484 antibodies were used: Mouse monoclonal anti-actin (Santa Cruz Biotechnology, sc-8432;
485 RRID:AB_626630); Mouse monoclonal anti- SOX18 (D-8) (Santa Cruz Biotechnology, sc-166025;
486 RRID:AB_2195662); Rat monoclonal anti- HHV-8 (LN-35) LANA (Abcam, ab4103; RRID:AB_304278);
487 Mouse monoclonal anti- KSHV K8.1 (Santa Cruz Biotechnology sc-65446; RRID:AB_831825); rabbit
488 monoclonal anti- GFP (a kind gift from J. Mercer; UCL, London, United Kingdom). Following HRP-
489 conjugated secondary antibodies were used: anti-mouse, anti-rabbit and anti-rat IgG HRP conjugated
490 (Cell Signaling Technology, 7076, 7074, 7077; RRID:AB_330924; RRID:AB_2099233;
491 RRID:AB_10694715).
492
493 **Viruses and infection**
494 wtKSHV inoculum was obtained from BCBL-1 cells (5x$10^5$ cells/ml) induced with 20 ng of TPA (12-*O*-
495 tetradecanoylphorbol-13-acetate; Sigma, St.Louis, USA)/ml. After 5 days, cells were pelleted, and the
496 supernatant was run through a 0.45 µm pore-size filter (Whatman, China). Virions were pelleted at
497 30,000xg for 2 h in a JA-14 rotor, Avanti-J-25 centrifuge (Beckman Coulter, Palo Alto, USA). The viral

pellet was resuspended in EBM-2 without supplements. wtKSHV infections were performed in serum-free EBM-2 supplemented with 8 μg/ml polybrene for 3 h, after which the medium was replaced with complete EBM-2 with supplements. Mock infections were performed identically except that concentrated virus was omitted from the inoculum.

The concentrated virus preparation of recombinant KSHV.219 virus was produced from iSLK.219 [34] as described in [12] and stored at -80°C. Cells infected with rKSHV.219 express green fluorescent protein (GFP) from the constitutively active human elongation factor 1-α (EF-1α) promoter and red fluorescent protein (RFP) under the control of RTA-responsive polyadenylated nuclear (PAN) promoter, expressed only during lytic replication. Cells were infected at low MOI 1-2 in EBM-2 media with supplements in the presence of 8 μg/mL polybrene (Sigma-Aldrich, St.Louis, USA) and spinoculation at 450g for 30 min, RT. Mock infections were performed identically except that concentrated virus was omitted from the inoculum.

**Virus release assay**

One day prior to titration, $8x10^3$ naïve U2OS cells/well were plated on viewPlate-96black (Perkin Elmer, Waltham, USA). Cells were spinoculated in the presence of 8 μg/mL of polybrene with serial dilution of precleared supernatant from infected LEC, BEC or ECFC cells. Cells were stained with antibodies against GFP (a kind gift from J. Mercer; UCL, London, United Kingdom) to detect the rKSHV.219-infected cells or LANA (ab4103; Abcam, Cambridge, UK) and Hoechst 33342 (Sigma-Aldrich, St.Louis, USA). Images were taken using automated cell imaging system ImageXpress Pico (Molecular Devices, San Jose, USA) and KSHV+ cells were quantified using pipeline created in CellProfiler (Broad Institute, Cambridge, USA).

520

521 **siRNA transfections**

522 Transient transfection of siRNA of a semi-confluent culture of KSHV-infected lymphatic ECFCs was done
523 using 3 µl of Lipofectamine RNAiMAX (Invitrogen, Lithuania) and 150 pmol siRNA in a 6-well plate
524 according to manufacturer's instructions. Next day cells were supplied with fresh media. The following
525 siRNAs were used: ON-TARGETplus SOX18 siRNA (L-019035-00); ON-TARGETplus Nontargeting pool
526 siRNA (D-001810-10) from Dharmacon (Lafayette, USA).

527

528 **Cell proliferation and viability**

529 Blood and lymphatic ECFCs were mock- or KSHV-infected. 48 hours post infection, $3x10^4$ cells/well were
530 seeded in 6-well dishes and imaged using an IncuCyte live cell imaging system (Essen Bioscience). Cell
531 confluence of 3 replicate wells was determined every hour for the duration of the experiment and 2
532 biological replicate experiments were performed.

533

534 To compare the proliferation rates of mock- and KSHV-infected lymphatic ECFCs, $5x10^3$ cells/well were
535 plated 5 days post infection on viewPlate-96black and the next day the cells were treated with 10 µM
536 5-ethynyl-2'-deoxyuridine EdU (Thermo Fisher, Eugene, OR) for 4 h and fixed in 4% paraformaldehyde
537 in PBS. The proliferating cells were visualized using EdU ClickIT (Invitrogen) staining according to
538 manufacturer's instructions, and Hoechst 33342. Images were taken using automated cell imaging
539 system ImageXpress Pico and the portion of EdU-containing cells was quantified with CellProfiler
540 software.

541

For measuring the viability of infected cells in serum and/or growth factor deprived media over time, CellTiter-Glo (Promega) assay was performed on 96-well plates for 20 min seeded with $5x10^3$ cells/well of each cell type in 8 corresponding wells and the luminescence from live cells were measured with FLUOstar Omega microplate reader (BMG Labtech, Mölndal, Sweden). The viability was calculated as an average of luminescent signal from 8 wells and presented as relative values.

**Tube formation of endothelial cells**

Matrigel (10 mg/ml; BD Biosciences, Bedford, MA) was applied at 0.5 ml/35 mm in a tissue culture dish and incubated at 37°C for at least 30 min to harden. Mock- or KSHV-infected cells were removed using trypsin-EDTA and resuspended at $1.5×10^5$ cells /ml in EBM-2 with supplements. Cells (1 ml) were gently added to Matrigel (Corning) -coated dish. Cells were incubated at 37°C, monitored for 4-24 h, and photographed in digital format using a Nikon microscope. Capillaries were defined as cellular processes connecting two bodies of cells. Ten fields of cells were counted for each condition and the mean and standard deviations were determined.

**Soft-agar assay**

Cells ($3x10^4$ /well) were mixed with 0.4% agarose as single cell suspension in growth medium and plated on top of a solidified layer of 0.5% agarose in EBM-2 with supplements in 6-well dishes. Fresh media was replenished every 2-3 days and wells were imaged each week using a BZ-X800 (Keyence) or Eclipse Ts2 (Nikon) fluorescent microscopes.

**RNA-sequencing**

564 Total RNA was isolated from mock- and KSHV-infected blood or lymphatic ECFCs using the NucleoSpin
565 RNA kit (Macherey-Nagel, Düren, Germany). RNA was further concentrated and purified using the RNA
566 Clean and Concentrator kit (Zymo Research, Irvine, CA). Purified RNA samples were processed at the
567 Fred Hutchison Cancer Research Center Genomic Resources core facility (Seattle, WA) and sequenced
568 using an Illumina HiSeq 2000. Image analysis and base calling were performed using RTA v1.17 software
569 (Illumina, San Diego, CA). Reads were aligned to the Ensembl's GRCh37 release 70 reference genome
570 using TopHat v2.08b and Bowtie 1.0.0 [40,41]. Counts for each gene were generated using htseq-count
571 v0.5.3p9. Differentially expressed genes were determined using the R package EdgeR (Bioconductor).
572 Genes were called significant with a |logFC| > 0.585 and a false discovery rate (FDC) of <0.05. Gene
573 Ontology enrichment was performed using Cytoscape and BINGO [42]. Using cytoscape software and
574 the Gene Ontology classification application BINGO, we determined the Gene Ontology terms that were
575 highly enriched among the blood and lymphatic specific expressed genes. The most highly enriched
576 categories for each cell type are listed in S1 & S3 Tables. Additionally, the data discussed in this
577 publication have been deposited in NCBI's Gene Expression Omnibus [43] and are accessible through
578 GEO Series accession number GSE54416 and GSE207589
579 (http://www.ncbi.nlm.nih.gov/geo/query/acc.cgi?acc=GSE54416
580 http://www.ncbi.nlm.gov/geo/query/acc.cgi?acc=GSE207589).
581
582 Total RNA was isolated from three independent experiments of the mock- and KSHV-infected lymphatic
583 ECFCs isolated as an adherent subpopulation from donor 1 using the NucleoSpin RNA extraction kit
584 (Macherey-Nagel), after which purity and concentration was determined with NanoDrop
585 spectrophotometer (Thermo Scientific). The RNA was sequenced in an Illumina Novaseq 6000 (150

586 bases, paired end) by Novogene (Cambridge, UK). Original image data was transformed to sequenced
587 reads by CASAVA base recognition. Raw data were cleaned from low quality reads and reads containing
588 adapter and poly-N-sequences in FASTP. Clean reads were mapped to the human genome
589 (GRCh38.p12) using HISAT2 with parameters—dta—phred33. Read counts were generated by
590 FeatureCounts [44]. Differentially expressed genes were determined using the R package DESeq2. The
591 resulting P values were adjusted using Benjamini and Hochberg's approach for controlling FDR. Genes
592 with adjusted P value <0.05 were assigned as differentially expressed. Raw data are deposited in NCBI's
593 Gene Expression Omnibus [43] and are accessible through GEO Series accession number GSE207657
594 (https://www.ncbi.nlm.nih.gov/geo/query/acc.cgi?acc=GSE207657).
595
596 **Quantitative RT-PCR**
597 Total RNA was isolated from cells using the RNeasy Plus Minikit (Qiagen, Maryland, USA) or NucleoSpin
598 RNA extraction kit (Macherey-Nagel) and used in quantitative reverse transcription PCR (RT-PCR;
599 Invitrogen, Van Allen Way Carlsbad, US) according to manufacturer's protocols. Real time quantitative
600 Polymerase chain reaction (RT-qPCR) and PrimePCR plates (Bio-Rad, Hercules, CA) or LightCycler480
601 PCR 384 multiwell plates (4titude FrameStar, Wotton, UK) were used to validate the RNA-Seq results.
602 Primer sequences used to amplify the indicated targets are listed in Table 1. Relative abundances of
603 viral mRNA were normalized by the delta threshold cycle method to the abundance of GAPDH or actin.
604
605 Table 1. Primers used in this study.

| **Primer** | **Forward primer** | **Reverse primer** |
|---|---|---|
| LANA | *ACTGAACACACGGACAACGG* | *CAGGTTCTCCCATCGACGA* |

| | | |
|---|---|---|
| K8.1 | *AAAGCGTCCAGGCCACCACAGA* | *GGCAGAAAATGGCACACGGTTAC* |
| ALU | *GGTGAAACCCCGTCTCTACT* | *GGTTCAAGCGATTCTCCTGC* |
| genomic actin | *AGAAAATCTGGCACCACACC* | *AACGGCAGAAGAGAGAACCA* |
| CD31 | *AACAGTGTTGACATGAAGAGCC* | *TGTAAAACAGCACGTCATCCTT* |
| VEGFC | *GCCAATCACACTTCCTGCCGA* | *AGGTCTTGTTCGCTGCCTGAC* |
| LYVE1 | *CTGCATGACACCTGGATGGA* | *AAGGGCTGGAAACAAGGACA* |
| Podoplanin | *CGAAGATGATGTGGTGACTC* | *CGATGCGAATGCCTGTTAC* |
| CD44 | *CCCATCCCAGACGAAGACAG* | *ACCATGAAAACCAATCCCAGG* |
| CD90 THY1 | *TCGCTCTCCTGCTAACAGTCT* | *CTCGTACTGGATGGGTGAACT* |
| aSMA | *GACCCTGAAGTACCCGATAGAAC* | *GGGCAACACGAAGCTCATTG* |
| ZEB1 | *GATGATGAATGCGAGTCAGATGC* | *ACAGCAGTGTCTTGTTGTTGTAG* |
| SNAI1 | *GCATTTCTTCACTCCGAAGC* | *TGAATTCCATGCTCTTGCAG* |
| ETS1 | *GAGCTTTTCCCCTCCCCGGAT* | *TGCCGGGGGTCTTTTGGGAT* |
| ETS2 | *AGGAGTTTCAGATGTTCCCC* | *GTCCCAGAATTGTTGGTGAG* |
| MMP1 | *AGTCCGGTTTTTCAAAGGGAA* | *CCTTGGGGTATCCGTGTAGC* |
| CXCR4 | *GCCAACGTCAGTGAGGCAGA* | *GCCAACCATGATGTGCTGAAAC* |
| IL6 | *GAACCTTCCAAAGATGGCTGA* | *CAAACTCCAAAAGACCAGTGATG* |
| TGFB3 | *TGAGCACATTGCCAAACAGC* | *ACTCAGTGGCAAAGCTAGGG* |
| actin | *TCACCCACACTGTGCCATCTACGA* | *CAGCGGAACCGCTCATTGCCAATGG* |
| GAPDH | *AAGGTGAAGGTCGGAGTCAAC* | *TGGAAGATGGTGATGGGATTTC* |
| Viperin | *GTGAGCAATGGAAGCCTGATC* | *GCTGTCACAGGAGATAGCGAGAA* |
| IFI6 | *CCTCGCTGATGAGCTGGTCT* | *CTATCGAGATACTTGTGGGTGGC* |
| IL1R1 | *AGAGGAAAACAAACCCACAAGG* | *CTGGCCGGTGACATTACAGA* |
| MyD88 | *GCACATGGGCACATACAGAC* | *GACATGGTTAGGCTCCCTCA* |

606

607 **Quantification of intracellular viral genome copies**

608 Total DNA was isolated from cells using NucleoSpin Tissue Kit 192 (Macherey-Nagel) and the KSHV
609 genome copies were quantified by qPCR using primers specific for LANA, K8.1, and genomic actin, listed
610 in Table 1.
611
612 **SOX18 inhibitor treatments *in vitro***
613 For the in vitro studies, small molecule SOX18 inhibitor SM4 (Sigma-Aldrich / or a kind gift from
614 Gertrude Biomedical Pty Ltd.) was solubilized in DMSO (Sigma-Aldrich) to obtain a stock solution of 50
615 µM and stored in 4°C.
616
617 For SOX18 inhibition in 3D spheroid cultures mock- or KSHV-infected lymphatic ECFCs were seeded into
618 0.5% agarose precoated, round-bottom 96-well plates (Corning, NY, USA) at $4x10^3$ cells per well. After
619 16-24 h incubation at 37°C, the preformed spheroids were transferred into the fibrin gel consisting of
620 plasminogen-free human fibrinogen (final concentration 3 mg/ml; Calbiochem, USA) and human
621 thrombin (final concentration 2 U/ml; Sigma) in 50 µl Hank's Balanced Salt Solution supplemented with
622 400 µg/ml aprotinin (Sigma). The gels were cast onto the bottom of 12-well plates and incubated for
623 1 h at 37°C to allow complete gelling followed by addition of EC culture medium. The next day, SM4 or
624 DMSO as a control was added to the culture media, replenished at day 3 and followed until day 6.
625 Images were taken and the spheroids were fixed with 4% PFA for 1 h RT. The spheroids were stained
626 by anti-rabbit GFP, and Hoechst 33342 as described in [10] and analyzed by confocal microscopy.
627
628 **In vivo model development and SOX18 inhibition**
629 Female NSG mice (Nonobese diabetic (NOD)/severe combined immunodeficiency (SCID); NOD.Cg-

630 Prkdc$^{scid}$ Il2rg$^{tm1Wjl}$/SzJ) used in this study were provided by Jackson Laboratory and acquired through
631 Scanbur (Germany). The mice were acclimatized for 7 days in isolation. After the isolation period, mice
632 were trained for handling, weighing and finally to oral gavage tube feeding with clean water to reduce
633 stress for the animals during the experimental procedures. The maintenance and all procedures with
634 the mice were performed in authorized facilities, at the Laboratory Animal Center University of Helsinki
635 (Finland), by trained certified researchers, and under a license approved by the national Animal
636 Experiment Board, Finland (license number ESAVI/10548/2019 for tumor growth and
637 ESAVI/22896/2020 for the oral gavage administration).
638
639 When the majority (about 90%) of the KSHV-infected lymphatic ECFCs expressed GFP, with some (about
640 5%) expressing RFP, the cells were collected and mixed with K-LECs, almost fully infected with
641 rKSHV.219, with a substantial part (20-30%) expressing RFP. The combined cell preparation consisted
642 of 90-95% of KSHV-infected lymphatic ECFCs and 5-10% of K-LECs. K-LECs were included to provide the
643 more spontaneously lytic cells that can contribute to the inflammatory microenvironment and produce
644 more infectious virus than the ECFCs. 5x10$^6$ cells/ 100 µL of cells were embedded in media containing
645 ice-cold growth-factor reduced Matrigel (Corning, NY, USA) at 3 mg/mL concentration. 100 µL of the
646 cell-Matrigel suspension was injected subcutaneously to the flanks of NSG mice, using total of 14 mice/
647 group.
648
649 For in vivo studies, SM4 was freshly prepared in the vehicle solution of 80% Kollisolv PEG-400 (Sigma-
650 Aldrich), 10% MilliQ water and 10% Kolliphor ELP/Solutol HS-15 (Sigma-Aldrich) for each treatment
651 dosing day at a concentration of 8 mg/mL. One day after subcutaneous implanting of the cell-Matrigel

652 suspension a dose of 25 mg/kg of body weight was administered to mice daily for 10 sequential days as
653 described in [27] using disposable polypropylene 20 ga, 38 mm feeding tubes (Instech, Philadelphia,
654 USA) optimal for safe intragastric (IG) administration. After the 10-day SM4 or Vehicle control
655 treatment, and 24h after the last dose, the mice were euthanatized under anesthesia by cervical
656 dislocation. The injected cells (appearing as visible/palpable Matrigel plugs) were quickly removed for
657 either histological sampling and embedded in 10% neutral buffered formalin solution (Sigma) or stored
658 in -80C for DNA extraction performed by NucleoSpin Tissue Kit (Macherey-Nagel) according to
659 manufacturer's instructions.
660
661 **Immunohistochemistry**
662 Deparaffination, rehydration and epitope revealing were done before staining as described in [38].
663 Sections were stained with Hematoxylin (Merck Millipore) and Eosin (Sigma-Aldrich) and with and
664 Immunofluorescence using anti-rabbit GFP antibody (a gift from Jason Mercer, University of
665 Birmingham, UK) and secondary anti-rabbit Alexa Fluor 488 antibody (Invitrogen). Nuclear staining was
666 done by incubating the sections in Hoechst 33342 (Sigma-Aldrich).
667
668 **Imaging and analysis**
669 H&E sections were imaged with automatic Panorammic250 slide scanner with 20x microscope through
670 services from Genome Biology Unit (GBU, University of Helsinki, Finland). Immunofluorescence images
671 from whole mount sections were taken with Zeiss Confocal LSM 780 microscope provided by
672 Biomedicum Imaging Unit (BIU, University of Helsinki, Finland). The images were taken as a Z-stack and
673 tiling was chosen to image the whole section area. Hoechst and GFP were imaged with 20x objective

674 using lasers Diode 405nm and Argon 488nm, respectively. The images were quantified by integrated
675 ZEN 3.5 analysis program (Zeiss, Germany) and a pipeline was generated for the images to measure the
676 relative GFP intensity normalized with the section area and the comparable coverage of the GFP signal
677 in the cells showing an elongated spindling phenotype.
678
679 **Statistical analysis**
680 Graphical presentations and statistical analysis were generated with GraphPad Prism Software v8.0
681 (Dotmatics, San Diego, USA). For statistical evaluation of the RT-qPCR data for relative KSHV genome
682 copies, the logarithmic values were converted to linear log2 scale values by using the double delta CT
683 (2-ΔΔ CT) method. Human ALU-sequences were used as internal control and accounted in the
684 calculations to correct differences in the DNA amount, quality, and PCR synthesis efficacy between the
685 samples. The data is presented as individual values ± standard deviation (SD) between biological
686 replicates. Statistical differences between groups were evaluated with Student's *t*-test (two-tailed).
687 Mean ± SD was shown and a p-value of ≤0.05 was considered significant and indicated by asterisk.
688
689 **Figure Legends**
690 **Figure 1. Lymphatic ECFCs are more permissive to KSHV infection than blood ECFCs and maintain the**
691 **KSHV viral episome. A.** Lymphatic and blood ECFCs were infected with KSHV (K-ECFCLY and K-ECFCBL
692 respectively) at either a high MOI (upper panel) or **B.** a low MOI (lower panel). At 48 h.p.i cells were
693 harvested and stained with anti-LANA antibody for the number of infected cells and DAPI for the
694 number of total cells. Cells were counted and the percentage of LANA+ cells was determined. These
695 experiments were performed with cells isolated from at least two different donors for each cell type.

**C.** KSHV-infection of lymphatic ECFCs, LECs and BECs was compared over 14 days and pictures shown at 7 d.p.i of spindling phenotype, latent infection (GFP) and spontaneous lytic replication (indicated by RFP expression). **D.** Expression of KSHV latent (LANA) and lytic (K8.1) proteins, in addition to GFP and SOX18 were analysed from mock- and infected lymphatic ECFCs. **E**. KSHV titers were measured by a virus release assay on naïve U2OS cells. **F.** Lymphatic (squares) and blood (circles) ECFCs were infected with KSHV and harvested every 2 days and stained for LANA expression. The percentage of LANA+ cells was determined. **G.** Lymphatic ECFCs (squares), K-LECs (triangles) and K-BECs (circles) were KSHV-infected at similar MOI and total DNA was collected at 3, 7, 10 and 14 d.p.i. Relative KSHV genome copies were determined. Experiments were performed three times with similar results. * $p < 0.05$, *** $p < 0.001$, **** $p < 0.0001$.

**Figure 2. KSHV inhibits proliferation but not capillary morphogenesis. A.** 48 hours after infection with KSHV, ECFCLY (squares), ECFCBL (circles), K-ECFCLY (upside down triangles) and K-ECFCBL (triangles), were seeded in 6-well dishes and placed in an Essen Biosciences IncuCyte. Pictures were taken every 2 hours and percentage confluence was determined. **B, C.** Mock- or KSHV-infected lymphatic ECFCs were seeded 5 d.p.i on 96-well dishes and **B.** treated with EdU for 4h before fixing. EdU-positive cells were stained, and percentages of proliferating cells were determined. **C.** Relative viability after 7 days in full or serum and/or growth factor deprived media was measured with CellTiter-Glo luminescence assay. **D.** Blood and lymphatic ECFCs were mock- or KSHV-infected. 48 h.p.i cells were plated on Matrigel and monitored for capillary morphogenesis at 4 and 24 hours post plating. * $p < 0.05$.

717 **Figure 3. KSHV confers a survival advantage to lymphatic ECFCs grown in soft agar. A.** Mock or KSHV-
718 infected lymphatic and blood ECFCs were embedded 48 h.p.i in soft agar overlaid with 0.5ml growth
719 media, and media was replenished every 2-4 days. **B.** The number of colonies with two or more cells at
720 36 days post plating were quantified. These experiments were performed up to eight times with similar
721 results. **C.** Lymphatic ECFCs mock- or KSHV- infected were embedded 5 d.p.i. in soft agar. iSLK.219 was
722 used as a positive control cell line. Quantification of number of colonies of at least 3 cells **(D)** and
723 number of cells in colonies from 4 different donors **(E)**. Experiments were performed at least three
724 times with similar results. ** $p < 0.01$.
725
726 **Figure 4. SM4 inhibit the hallmarks of KSHV infection in lymphatic ECFCs in vitro.** Lymphatic ECFCs
727 were infected with KSHV for 5 days, and treated with **A-E.** siRNA targeting SOX18, or control siRNA
728 (siNeg) transfected for 72h or **E-H.** with indicated concentrations of SM4 inhibitor or DMSO control for
729 6 days, replenished at day 3. The effect of treatments is shown as quantified **A, F.** KSHV genome copies
730 from total DNA, **B, G.** percent of LANA positive cells on 96-well plates and **C, H.** KSHV titers measured
731 from virus release assay on naïve U2OS cells. **D.** The efficiency of SOX18 silencing shown at a protein
732 level. **E.** Changes in spindling morphology, GFP (latent) and RFP (lytic) cells shown with siRNA targeting
733 SOX18 or 25 µM of SM4 and DMSO control. **I-J.** Lymphatic ECFCs were either mock or KSHV-infected,
734 allowed to form spheroids overnight and then embedded in 3D fibrin. Spheroids were treated for 6-
735 days with 50 µM of SM4 or DMSO control, and fixed. Phase contrast and confocal images are shown at
736 treatment day 6. * $p < 0.05$, ** $p < 0.01$, *** $p < 0.001$.
737

738 **Figure 5. SM4 inhibit the hallmarks of KSHV infection in lymphatic ECFCs in vivo. A.** Schematic of the
739 experimental in vivo layout of SOX18 inhibition on ECFCLY KSHV-infection model and sample collection.
740 **B.** Lymphatic ECFCs infected with KSHV for 7 days, or left uninfected, were implanted subcutaneously
741 to NSG mice. Long-term persistence of K-ECFCLY seen as expression of spindling GFP-positive cells and
742 staining of nuclear LANA dots, not seen with uninfected ECFCLY, from grafts extracted 30 days post
743 implantation. **C-E.** Lymphatic ECFCs and LECs, infected with KSHV for 7 days, or left uninfected, were
744 implanted subcutaneously to NSG mice with ratio of 90-95% of K-ECFCs and 5-10% of K-LECs. 24h post
745 implantation the mice were treated with either SM4 or Vehicle control daily for 10 days after which
746 mice were sacrificed and grafts were collected for total DNA and IHC. **C.** H&E staining imaged with slide
747 scanner and GFP imaged with confocal microscope. Quantification of **D.** overall GFP intensity, GFP
748 intensity only in spindling cells and spindling morphology (n = 12/ SM4 and 13/ Vehicle group) and **E.**
749 normalized KSHV genome copies from total DNA measured with RT-qPCR between SM4 or Vehicle
750 treated mice (n = 14/group). ** $p < 0.01$, *** $p < 0.001$.
751

# 752 Supporting information

753 **S1 Fig. Subpopulation of characterized ECFC isolates express markers of lymphatic vasculature.**
754 Comparison of adherent ECFCs isolate to mature LECs and BECs **A.** of the morphology, **B.** and expression
755 of surface and intracellular endothelial markers by FACS, **C.** measured also from isolates from 4 different
756 donors.
757

**S2 Fig. Comparison of infected lymphatic ECFCs from different donors**. ECFCLY isolated from 4 different donors, were infected with KSHV. **A.** Pictures taken at 7 d.p.i show spindling phenotype, latent infection (GFP) and spontaneous lytic replication (indicated by RFP expression). **B.** Expression of KSHV latent (LANA) and lytic (K8.1) proteins and SOX18 and **C.** KSHV titers were measured from virus release assay on naïve U2OS cells.

**S3 Fig. Gene expression changes induced by KSHV infection of lymphatic ECFCs.**

**A.** Venn diagram showing overlapping gene expression profiles of uninfected BEC and LEC along with blood and lymphatic ECFCs. **B, C.** Blood (black bars) and lymphatic (white bars) ECFCs were mock- or KSHV-infected. At 48 h.p.i, RNA was isolated and analyzed for gene expression of **B.** a selection of genes and of **C.** immune response genes identified as changed by RNA-sequencing. **D-F.** Lymphatic ECFCs were mock or KSHV-infected, and 7 d.p.i RNA was isolated and analyzed for gene expression by RNA-sequencing. Common gene expression changes between different isolates of ECFCLY after KSHV-infection are shown as Venn diagram **(D)**. Volcano blot with at least 2-fold up- (orange) and downregulated (black) genes with adjusted P value < 0.05 **(E),** and validation of selection of genes by qPCR **(F).** RNA-sequencing was done with biological triplicates of each sample.

**S Table 1. Gene Ontology categories enriched in KSHV-infected blood ECFCs.**

**S Table 2. Gene Ontology category genes enriched in KSHV-infected blood ECFCs.**

**S Table 3. Gene Ontology categories enriched in KSHV-infected lymphatic ECFCs.**

**S Table 4. Gene Ontology category genes enriched in KSHV-infected lymphatic ECFCs.**

**S Table 5. Differentially expressed genes between blood and lymphatic ECFCs.**

**S table 6. Shared differentially expressed genes between K-ECFCLYs 7d and 48h post infection.**

**Author Contributions:**

K.T. and T.A.D. designed the study, performed experiments, analyzed the data, and wrote the manuscript. E.A.K., P.S., and P.L. provided research material, technical advice and contributed to the writing of the manuscript. T.K. provided expert advice, funding and contributed to the writing of the manuscript. M.L. and P.M.O. designed the study, analyzed the data, contributed to the writing of the manuscript, and provided funding.

# Acknowledgements

We thank the Laboratory Animal Center (LAC), Biomedicum Imaging Unit (BIU), and Genome Biology Unit (GBU) at the University of Helsinki for support in animal care and imaging. We are also extremely grateful to Nadezhda Zinovkina, Hector Monzo, Shadi Azam and Vadim Le Joncour (University of Helsinki) for the valuable technical help. Mathias Francoís (The Centenary Institute, University of Sydney, Australia) is acknowledged for valuable comments for the manuscript.

# References

1. Jussila L, Valtola R, Partanen TA, Salven P, Heikkilä P, Matikainen MT, et al. Lymphatic endothelium and Kaposi's sarcoma spindle cells detected by antibodies against the vascular endothelial growth factor receptor-3. Cancer Res. 1998 Apr 15;58(8):1599–604.
2. Skobe M, Brown LF, Tognazzi K, Ganju RK, Dezube BJ, Alitalo K, et al. Vascular Endothelial Growth Factor-C (VEGF-C) and its Receptors KDR and ¯t-4 are Expressed in AIDS-Associated Kaposi's Sarcoma.
3. Weninger W, Partanen TA, Breiteneder-Geleff S, Mayer C, Kowalski H, Mildner M, et al. Expression of vascular endothelial growth factor receptor-3 and podoplanin suggests a

lymphatic endothelial cell origin of Kaposi's sarcoma tumor cells. Lab Invest. 1999 Feb;79(2):243–51.

4. Reis RM, Reis-Filho JS, Filho AL, Tomarev S, Silva P, Lopes JM. Differential Prox-1 and CD 31 expression in mucousae, cutaneous and soft tissue vascular lesions and tumors. Pathology Research and Practice. 2005 Dec 14;201(12):771–6.
5. Regezi JA, Macphail LA, Daniels TE, Desouza YG, Greenspan JS, Greenspan D. Human Immunodeficiency Virus-Associated Oral Kaposi's Sarcoma A Heterogeneous Cell Population Dominated by Spindle-Shaped Endothelial Cells. Vol. 143, American Journal of Pathologv. 1993.
6. Carroll PA, Brazeau E, Lagunoff M. Kaposi's sarcoma-associated herpesvirus infection of blood endothelial cells induces lymphatic differentiation. Virology. 2004 Oct 15;328(1):7–18.
7. Hong YK, Foreman K, Shin JW, Hirakawa S, Curry CL, Sage DR, et al. Lymphatic reprogramming of blood vascular endothelium by Kaposi sarcoma-associated herpesvirus. Nature Genetics. 2004 Jul;36(7):683–5.
8. Wang HW, Trotter MWB, Lagos D, Bourboulia D, Henderson S, Mäkinen T, et al. Kaposi sarcoma herpesvirus-induced cellular reprogramming contributes to the lymphatic endothelial gene expression in Kaposi sarcoma. Nature Genetics. 2004 Jul;36(7):687–93.
9. Li Y, Zhong C, Liu D, Yu W, Chen W, Wang Y, et al. Evidence for Kaposi sarcoma originating from mesenchymal stem cell through KSHV-induced mesenchymal-to-endothelial transition. Cancer Research. 2018 Jan 1;78(1):230–45.
10. Cheng F, Pekkonen P, Laurinavicius S, Sugiyama N, Henderson S, Günther T, et al. KSHV-initiated notch activation leads to membrane-type-1 matrix metalloproteinase-dependent lymphatic endothelial-to-mesenchymal transition. Cell Host and Microbe. 2011 Dec 15;10(6):577–90.
11. Gasperini P, Espigol-Frigole G, McCormick PJ, Salvucci O, Maric D, Uldrick TS, et al. Kaposi sarcoma herpesvirus promotes endothelial-to-mesenchymal transition through notch-dependent signaling. Cancer Research. 2012 Mar 1;72(5):1157–69.
12. Gramolelli S, Elbasani E, Tuohinto K, Nurminen V, Günther T, Kallinen RE, et al. Oncogenic Herpesvirus Engages Endothelial Transcription Factors SOX18 and PROX1 to Increase Viral Genome Copies and Virus Production. Cancer Research. 2020 Aug 1;80(15):3116–29.
13. Choi D, Park E, Kim KE, Jung E, Seong YJ, Zhao L, et al. The Lymphatic Cell Environment Promotes Kaposi Sarcoma Development by Prox1-Enhanced Productive Lytic Replication of Kaposi Sarcoma Herpes Virus. Cancer Res. 2020;80(15):3130–44.
14. DiMaio TA, Vogt DT, Lagunoff M. KSHV requires vCyclin to overcome replicative senescence in primary human lymphatic endothelial cells. PLOS Pathogens. 2020 Jun 18;16(6):e1008634.
15. Chang HH, Ganem D. A Unique Herpesviral Transcriptional Program in KSHV-Infected Lymphatic Endothelial Cells Leads to mTORC1 Activation and Rapamycin Sensitivity. Cell Host & Microbe. 2013 Apr;13(4):429–40.

16. Asahara T, Murohara T, Sullivan A, Silver M, van der Zee R, Li T, et al. Isolation of putative progenitor endothelial cells for angiogenesis. Science. 1997 Feb 14;275(5302):964–7.
17. Le Ricousse-Roussanne S, Barateau V, Contreres JO, Boval B, Kraus-Berthier L, Tobelem G. Ex vivo differentiated endothelial and smooth muscle cells from human cord blood progenitors home to the angiogenic tumor vasculature. Cardiovasc Res. 2004 Apr 1;62(1):176–84.
18. Barozzi P, Luppi M, Facchetti F, Mecucci C, Alù M, Sarid R, et al. Post-transplant Kaposi sarcoma originates from the seeding of donor-derived progenitors. Nat Med. 2003 May;9(5):554–61.
19. Della Bella S, Taddeo A, Calabrò ML, Brambilla L, Bellinvia M, Bergamo E, et al. Peripheral blood endothelial progenitors as potential reservoirs of Kaposi's sarcoma-associated herpesvirus. PLoS One. 2008 Jan 30;3(1):e1520.
20. Yoo S, Kim S, Yoo S, Hwang IT, Cho H, Lee MS. Kaposi's sarcoma-associated herpesvirus infection of endothelial progenitor cells impairs angiogenic activity in vitro. J Microbiol. 2011 Apr;49(2):299–304.
21. Cancian L, Hansen A, Boshoff C. Cellular origin of Kaposi's sarcoma and Kaposi's sarcoma-associated herpesvirus-induced cell reprogramming. Trends Cell Biol. 2013 Sep;23(9):421–32.
22. DiMaio TA, Wentz BL, Lagunoff M. Isolation and characterization of circulating lymphatic endothelial colony forming cells. Experimental Cell Research. 2016 Jan;340(1):159–69.
23. Yoder MC, Mead LE, Prater D, Krier TR, Mroueh KN, Li F, et al. Redefining endothelial progenitor cells via clonal analysis and hematopoietic stem/progenitor cell principals. Blood. 2007 Mar 1;109(5):1801–9.
24. Salven P, Mustjoki S, Alitalo R, Alitalo K, Rafii S. VEGFR-3 and CD133 identify a population of CD34+ lymphatic/vascular endothelial precursor cells. Blood. 2003 Jan 1;101(1):168–72.
25. Tan Y zhen, Wang H jie, Zhang M hua, Quan Z, Li T, He Q zhi. CD34+ VEGFR-3+ progenitor cells have a potential to differentiate towards lymphatic endothelial cells. J Cell Mol Med. 2014 Mar;18(3):422–33.
26. Fontaine F, Overman J, Moustaqil M, Mamidyala S, Salim A, Narasimhan K, et al. Small-Molecule Inhibitors of the SOX18 Transcription Factor. Cell Chem Biol. 2017 Mar 16;24(3):346–59.
27. Overman J, Fontaine F, Moustaqil M, Mittal D, Sierecki E, Sacilotto N, et al. Pharmacological targeting of the transcription factor SOX18 delays breast cancer in mice. Elife. 2017;6.
28. Vieira J, O'Hearn PM. Use of the red fluorescent protein as a marker of Kaposi's sarcoma-associated herpesvirus lytic gene expression. Virology. 2004 Aug 1;325(2):225–40.
29. Aluigi MG, Albini A, Carlone S, Repetto L, de Marchi R, Icardi A, et al. KSHV sequences in biopsies and cultured spindle cells of epidemic, iatrogenic and Mediterranean forms of Kaposi's sarcoma. Research in Virology. 1996 Sep;147(5):267–75.
30. Lebbé C, de Crémoux P, Millot G, Podgorniak MP, Verola O, Berger R, et al. Characterization of in vitro culture of HIV-negative Kaposi's sarcoma-derived cells. In vitro responses to alfa interferon. Arch Dermatol Res. 1997 Jun;289(7):421–8.

31. Lagunoff M, Bechtel J, Venetsanakos E, Roy AM, Abbey N, Herndier B, et al. De novo infection and serial transmission of Kaposi's sarcoma-associated herpesvirus in cultured endothelial cells. J Virol. 2002 Mar;76(5):2440–8.
32. Grundhoff A, Ganem D. Inefficient establishment of KSHV latency suggests an additional role for continued lytic replication in Kaposi sarcoma pathogenesis. J Clin Invest. 2004 Jan;113(1):124–36.
33. DiMaio TA, Gutierrez KD, Lagunoff M. Kaposi's sarcoma-associated herpesvirus downregulates transforming growth factor β2 to promote enhanced stability of capillary-like tube formation. J Virol. 2014 Dec;88(24):14301–9.
34. Myoung J, Ganem D. Generation of a doxycycline-inducible KSHV producer cell line of endothelial origin: maintenance of tight latency with efficient reactivation upon induction. J Virol Methods. 2011 Jun;174(1–2):12–21.
35. Crameri M, Bauer M, Caduff N, Walker R, Steiner F, Franzoso FD, et al. MxB is an interferon-induced restriction factor of human herpesviruses. Nat Commun. 2018;9(1):1980.
36. Schilling M, Bulli L, Weigang S, Graf L, Naumann S, Patzina C, et al. Human MxB Protein Is a Pan-herpesvirus Restriction Factor. J Virol. 2018;92(17).
37. Vogt D, Zaver S, Ranjan A, DiMaio T, Gounder AP, Smith JG, et al. STING is dispensable during KSHV infection of primary endothelial cells. Virology. 2020;540:150–9.
38. Mead LE, Prater D, Yoder MC, Ingram DA. Isolation and characterization of endothelial progenitor cells from human blood. Curr Protoc Stem Cell Biol. 2008 Jul;Chapter 2:Unit 2C.1.
39. Gramolelli S, Cheng J, Martinez-Corral I, Vähä-Koskela M, Elbasani E, Kaivanto E, et al. PROX1 is a transcriptional regulator of MMP14. Scientific Reports. 2018 Dec 1;8(1).
40. Trapnell C, Pachter L, Salzberg SL. TopHat: discovering splice junctions with RNA-Seq. Bioinformatics. 2009 May 1;25(9):1105–11.
41. Langmead B, Trapnell C, Pop M, Salzberg SL. Ultrafast and memory-efficient alignment of short DNA sequences to the human genome. Genome Biology. 2009;10(3):R25.
42. Saito R, Smoot ME, Ono K, Ruscheinski J, Wang PL, Lotia S, et al. A travel guide to Cytoscape plugins. Nature Methods. 2012 Nov 6;9(11):1069–76.
43. Edgar R, Domrachev M, Lash AE. Gene Expression Omnibus: NCBI gene expression and hybridization array data repository. Nucleic Acids Res. 2002 Jan 1;30(1):207–10.
44. Liao Y, Smyth GK, Shi W. featureCounts: an efficient general purpose program for assigning sequence reads to genomic features. Bioinformatics. 2014 Apr 1;30(7):923–30.

# Figure 1.

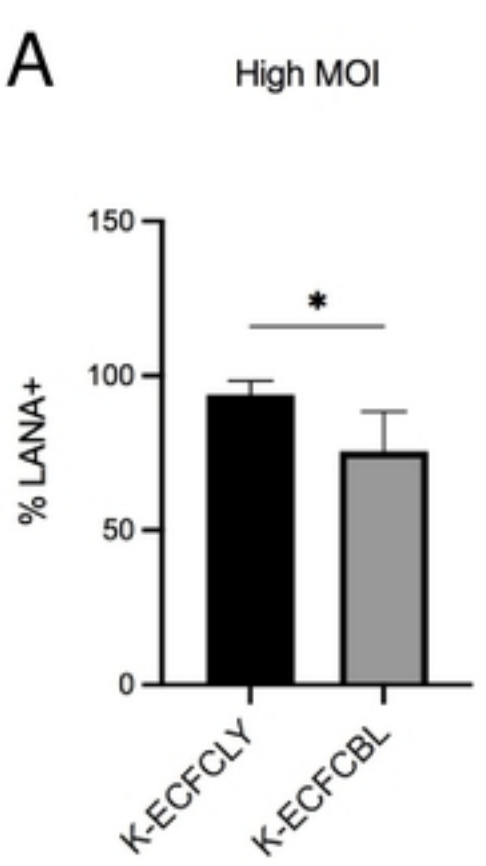


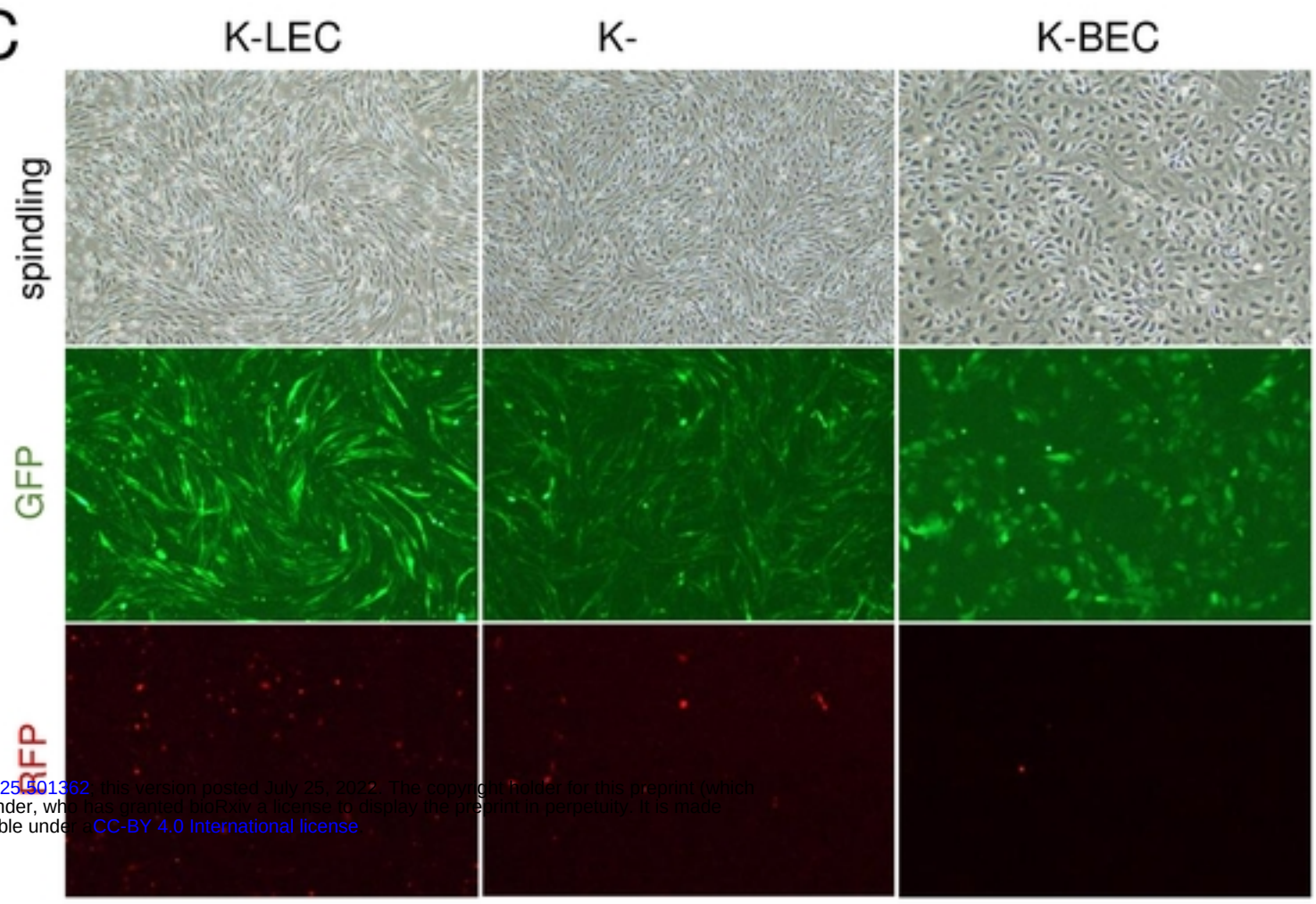




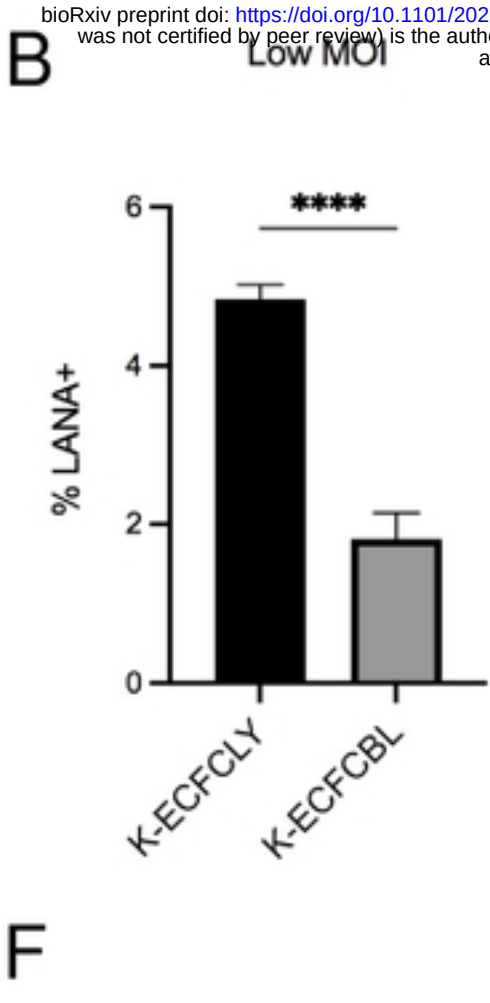


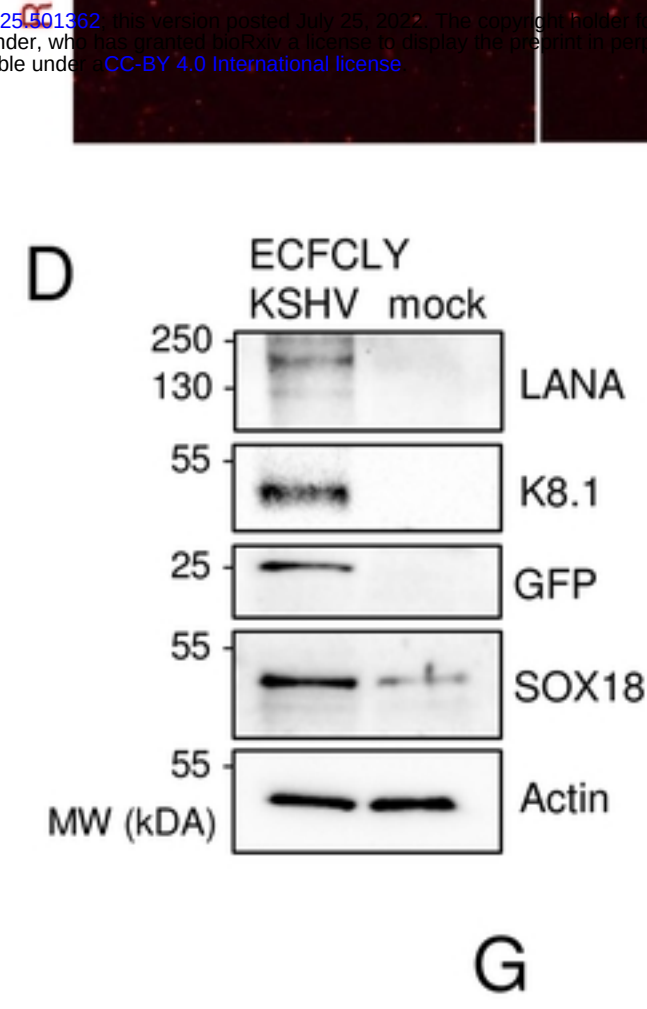


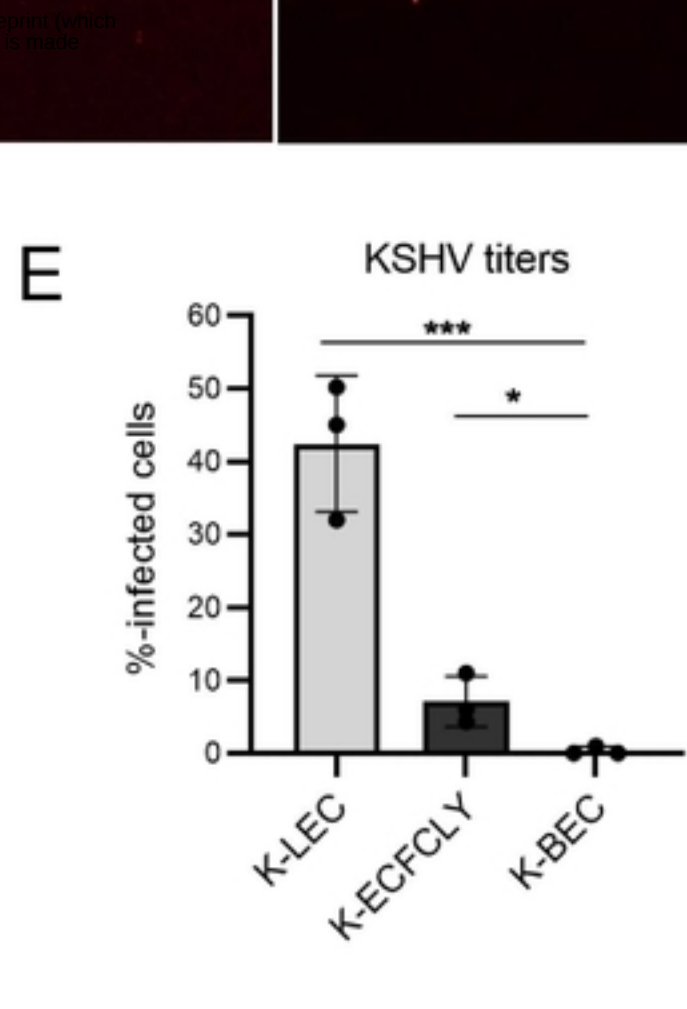


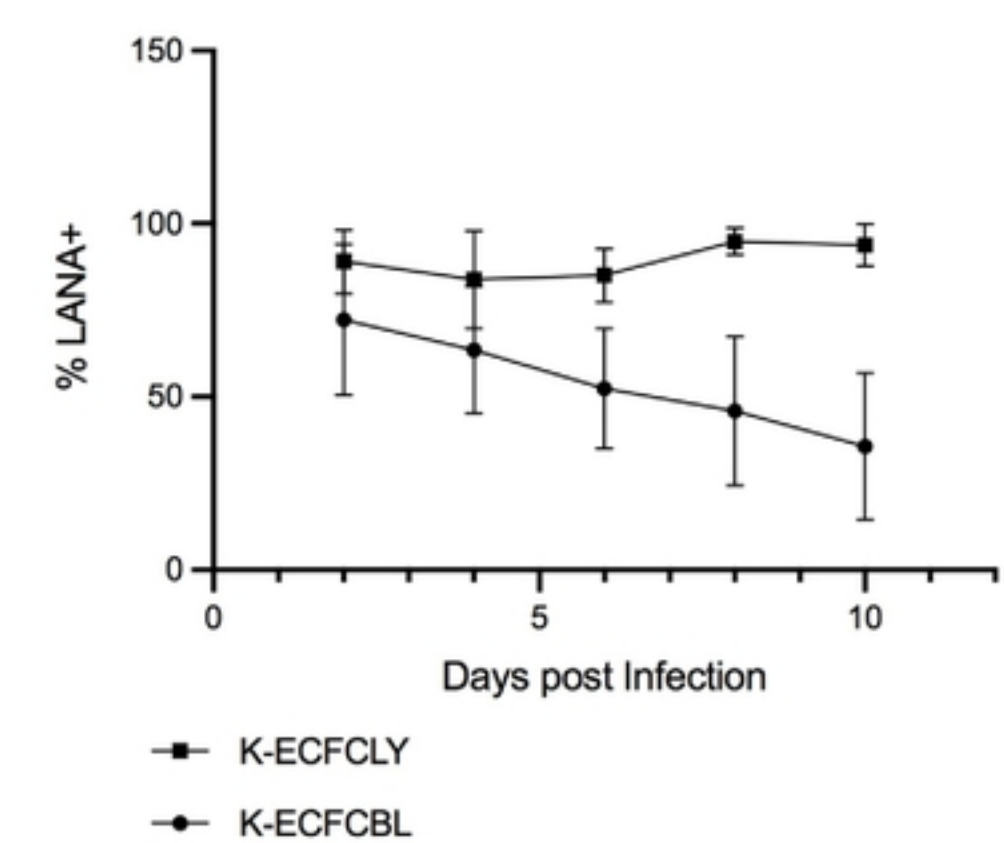


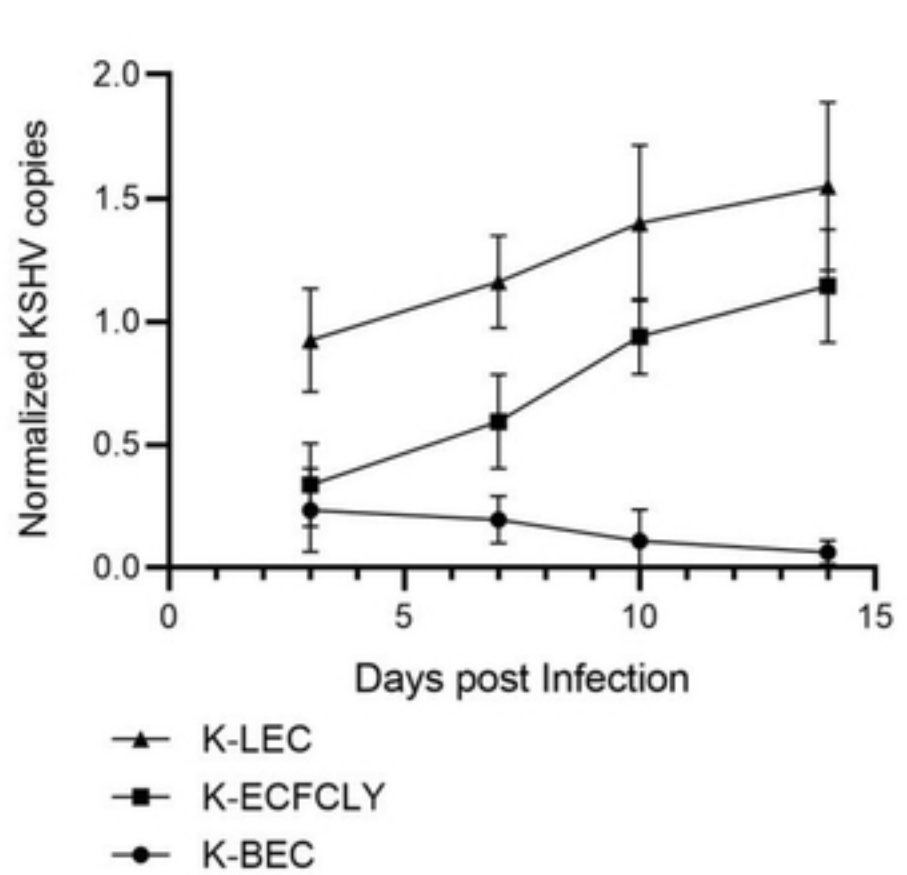

**Figure 2.**

A

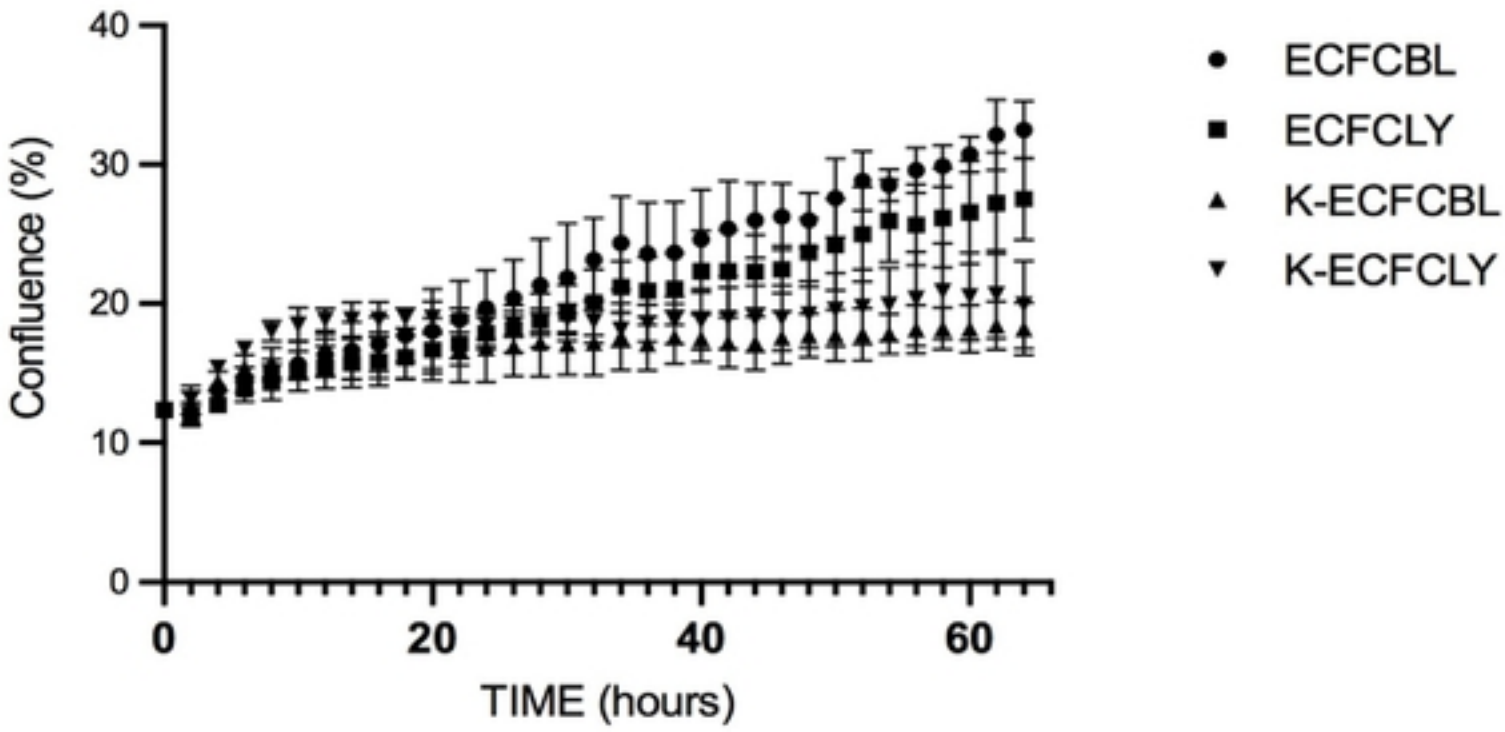




B

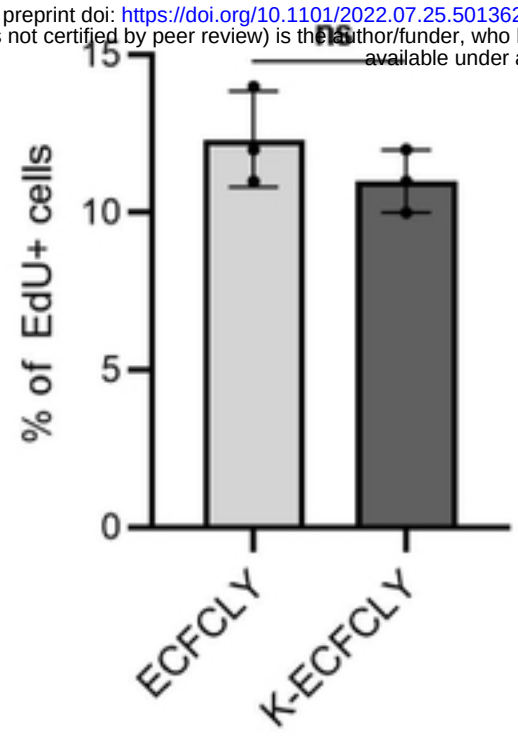


C

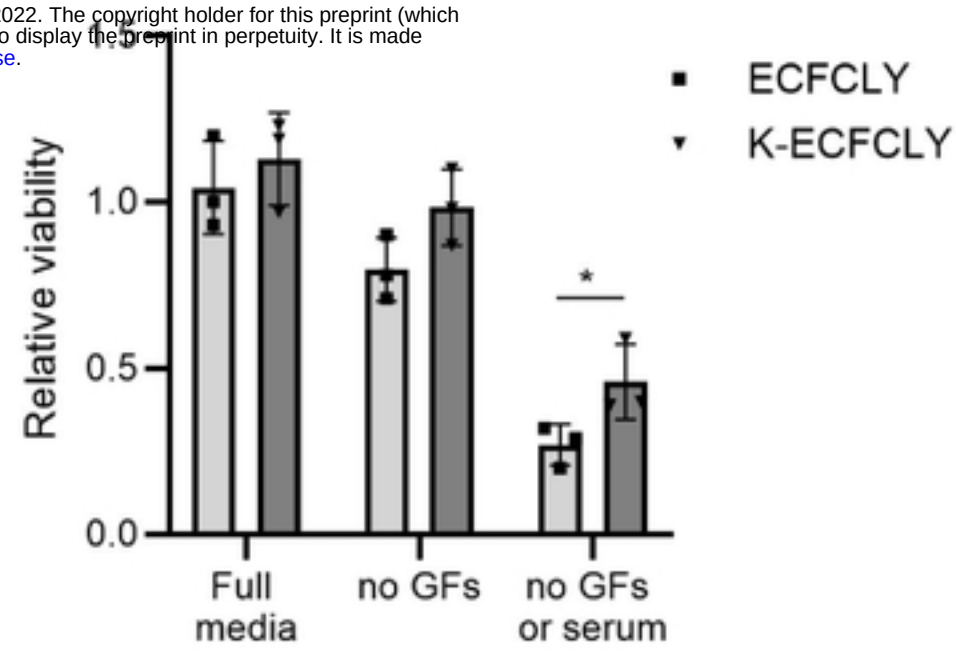


D

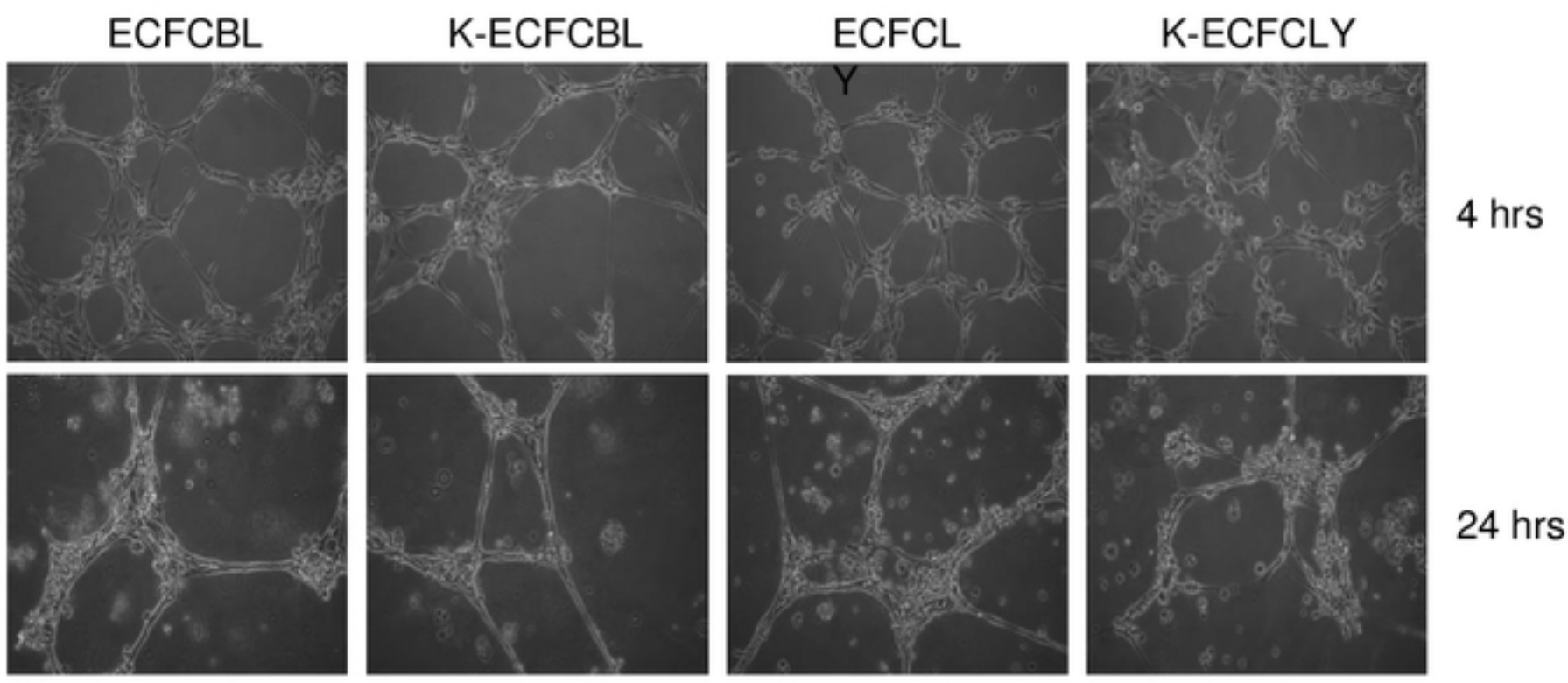

# Figure 3.

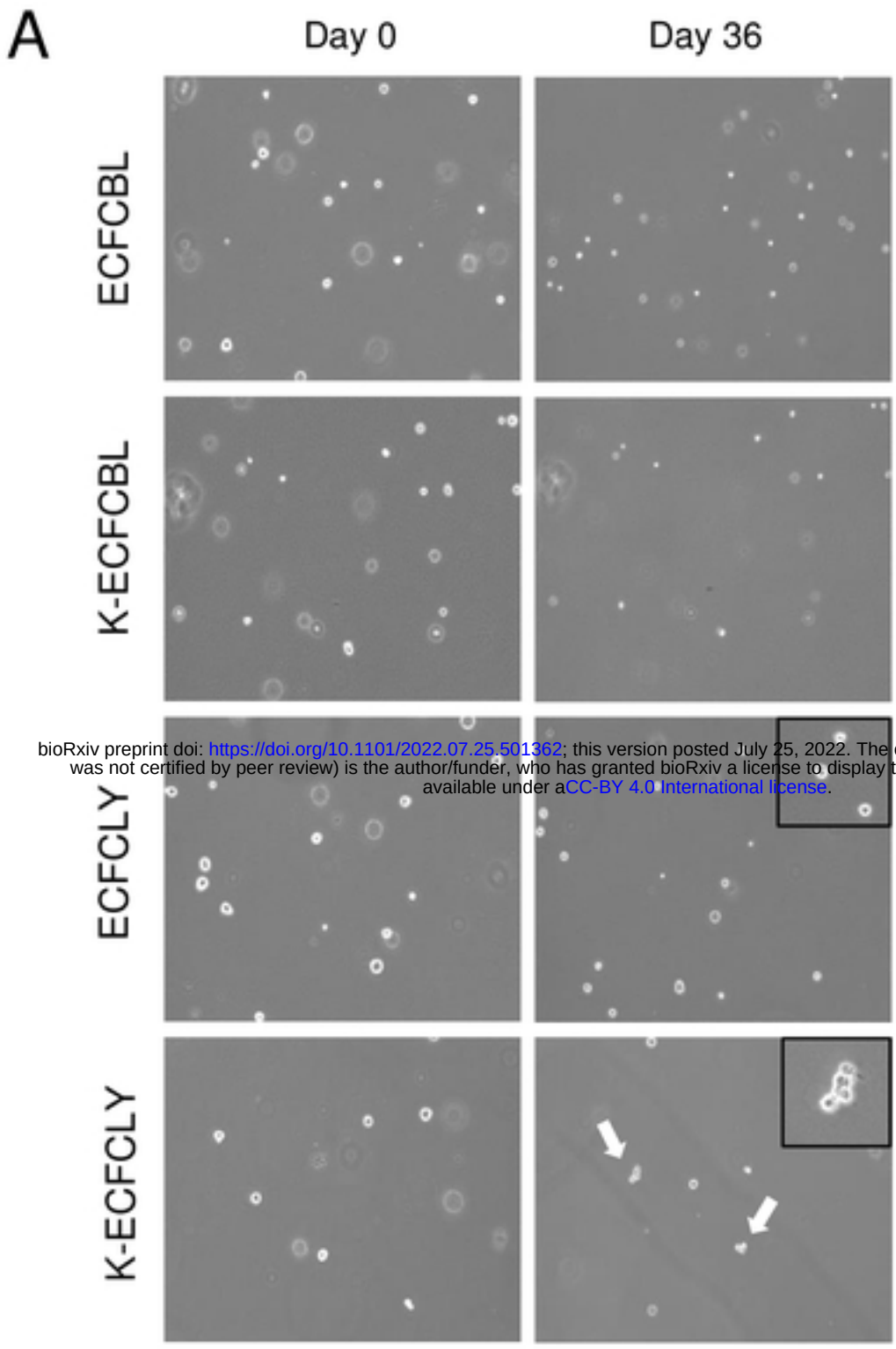




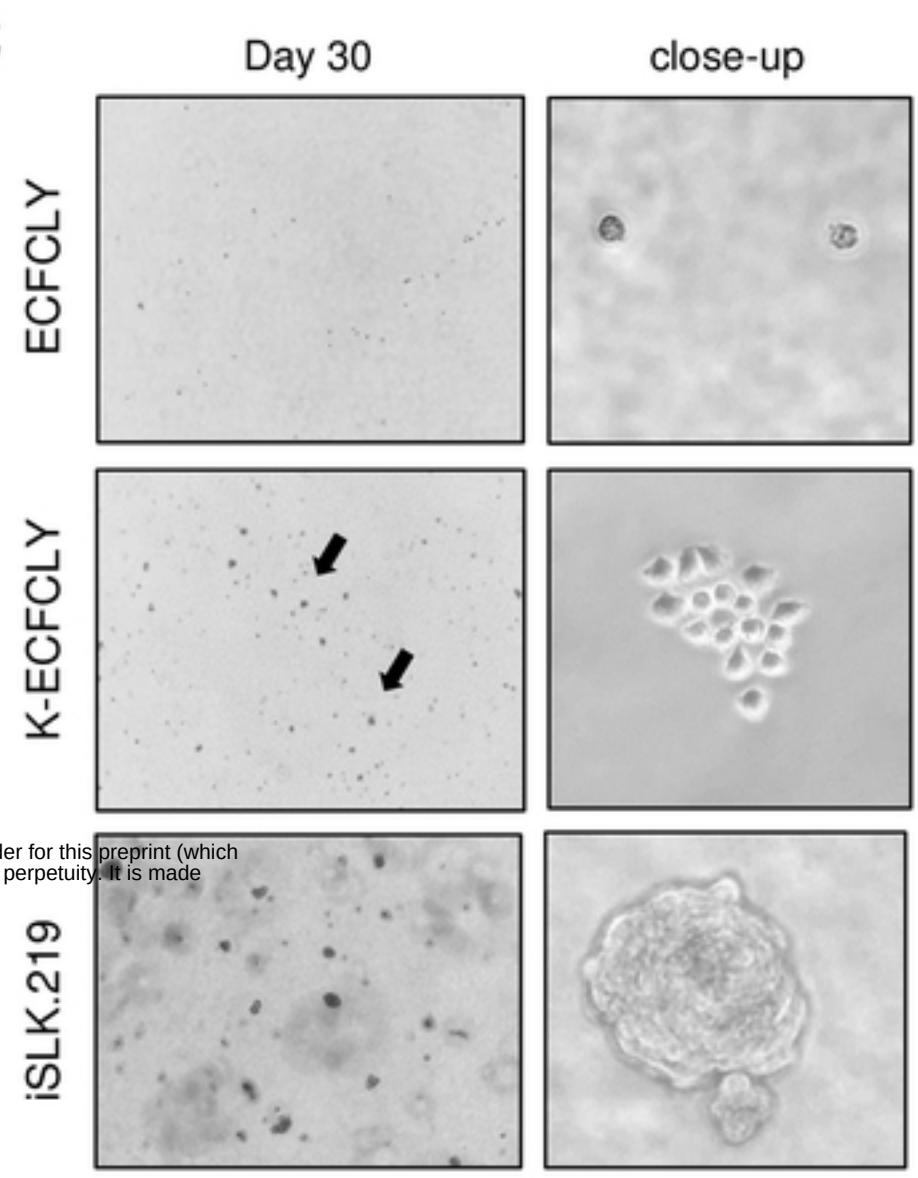


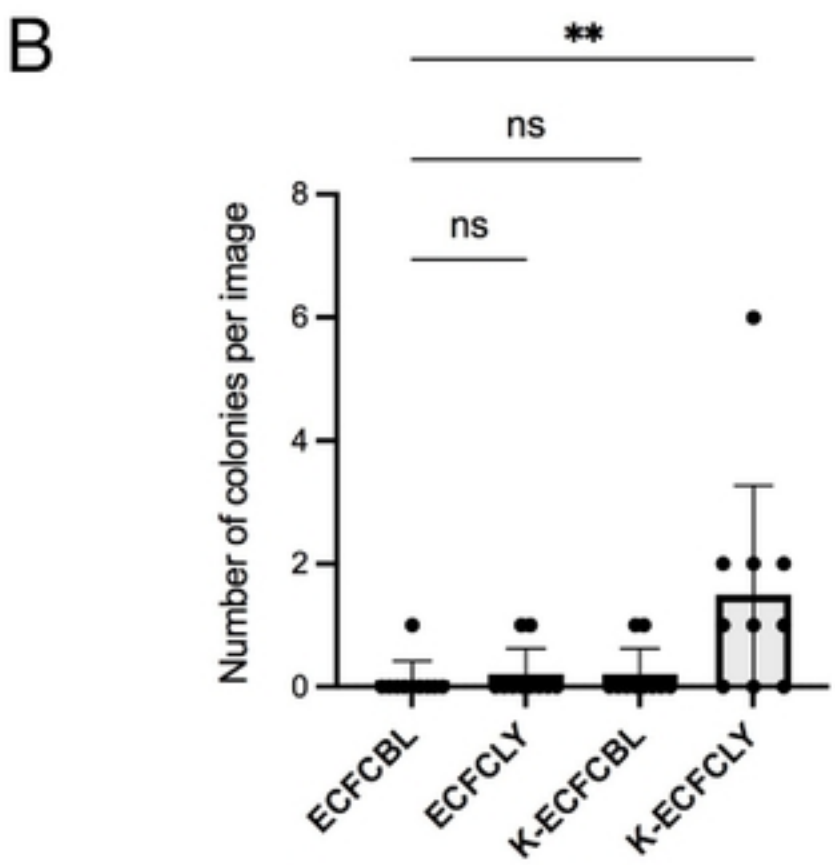


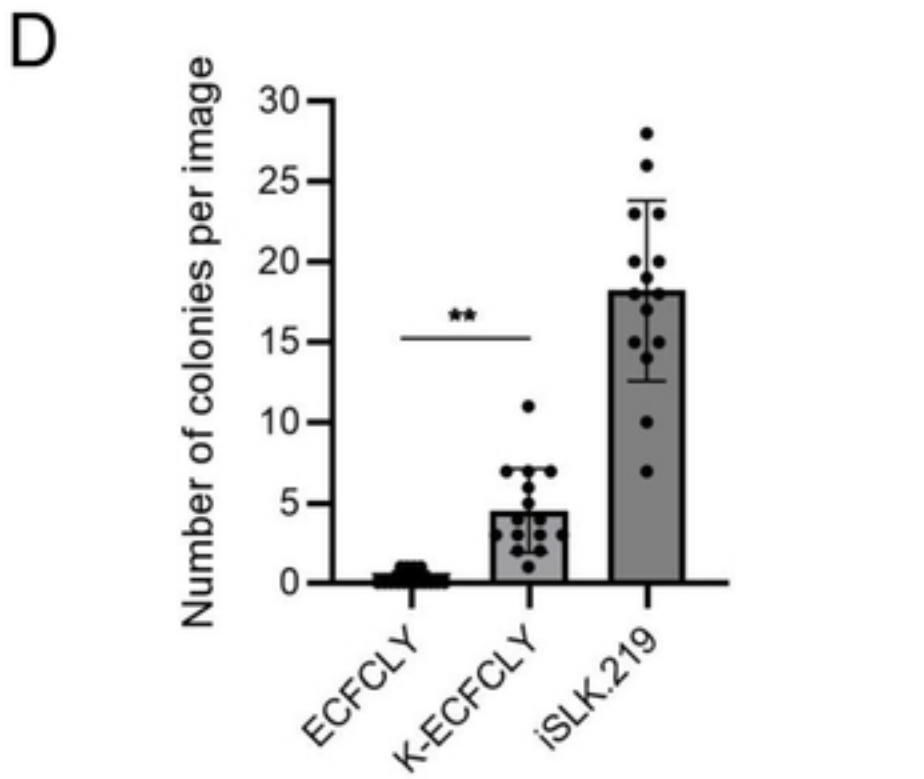


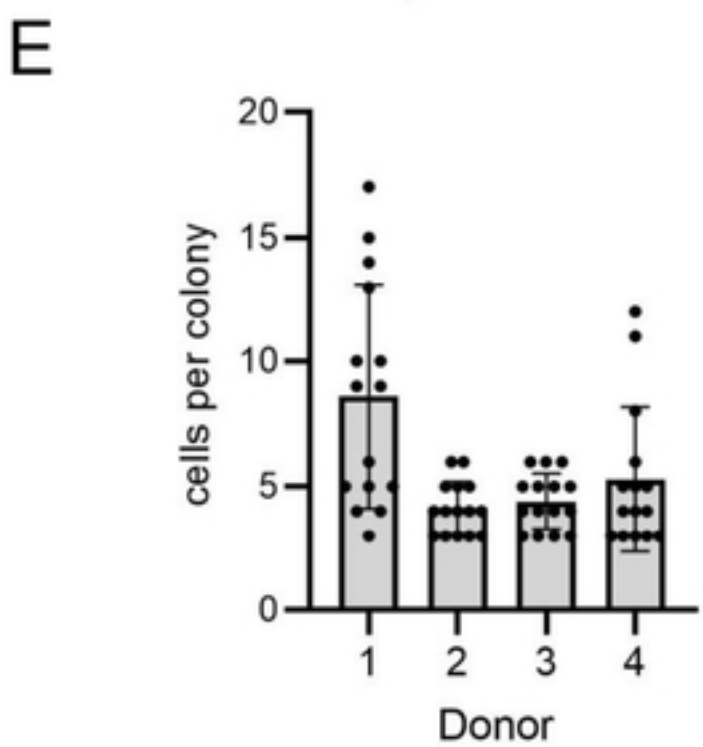

**Figure 4.**

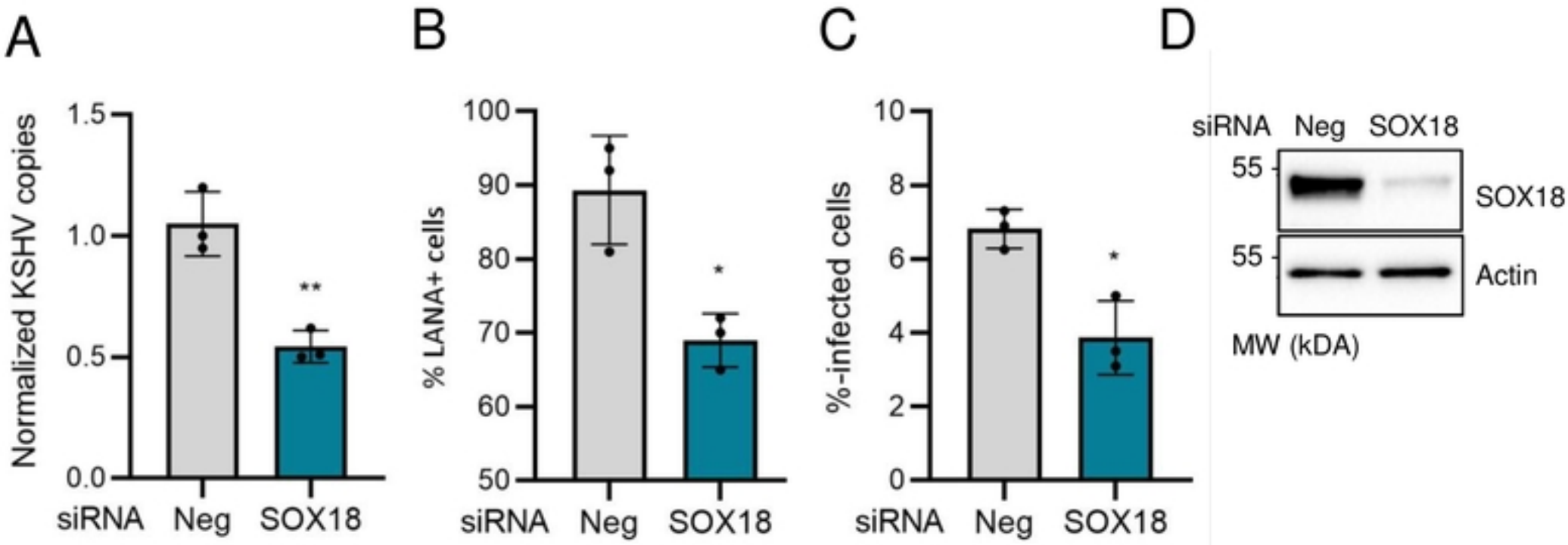

**Figure 4.** continued…

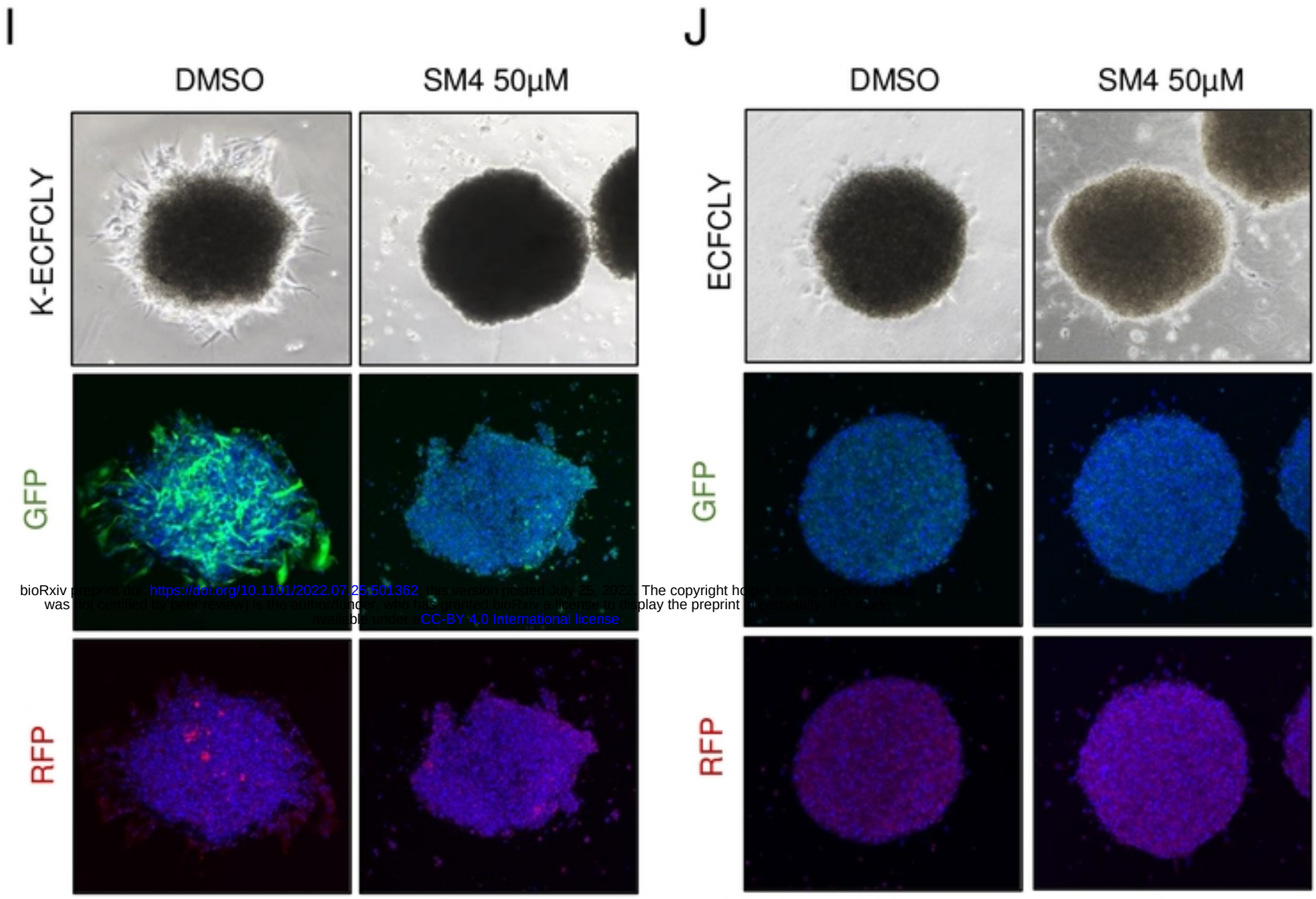

# Figure 5.